Marine Biodiversity (2021) 51:87
https://doi.org/10.1007/s12526-021-01216-6

SENCKENBERG

ORIGINAL PAPER

Distribution and diel vertical migration of mesopelagic fishes in the Southern Sargasso Sea — observations through hydroacoustics and stratified catches

L. Marohn[1] · M. Schaber[2] · M. Freese[1] · J. D. Pohlmann[1] · K. Wysujack[1] · S. Czudaj[2,3] · T. Blancke[1] · R. Hanel[1]

Received: 17 March 2021 / Revised: 14 July 2021 / Accepted: 15 July 2021

Abstract

Vertical distribution patterns and relative abundance of mesopelagic fish species and other major taxonomic groups were investigated through vertically stratified trawl sampling and hydroacoustic analyses along the subtropical convergence zone from 52° W to 70° W in the oligotrophic Sargasso Sea. Persistent stationary layers and several migrating components of different scattering characteristics were detected. The results reveal varying vertical migration patterns, including different times of onset of diel vertical migration in different depths and a migrant pathway emerging daily from the lower deep scattering layer (DSL) at dusk and migrating through the upper DSL without affecting its composition. Fish species identification was made based on morphological characteristics and confirmed by genetic barcoding analyses of subsamples. In total, 5022 fish specimens from 27 families, 62 genera and 70 species were caught. In terms of relative abundance (A) and biomass (M), catches were dominated by species of the families Myctophidae (A=59.1%, M=47.4% of total fish catch) and Melamphaidae (A=22.5%, M=17.1%). Myctophidae and Stomiidae were the most species-rich families with 31 and 12 species, respectively. Catches at the two easternmost stations were dominated by *Scopelogadus mizolepis* and *Nannobrachium cuprarium,* while *Bolinichthys photothorax* and *Ceratoscopelus warmingii* were the most abundant species in catches from the two westernmost stations. This study provides insights into distribution and vertical migration behaviour of mesopelagic fish in the Sargasso Sea and adds to our understanding of the mesopelagic community in this large oceanic area.

Keywords Pelagic ecology · Micronekton · Deep scattering layers · Western Atlantic

Introduction

Mesopelagic fish, living in depths of 200 to 1000 m, are dominating the fish biomass in large parts of the world's oceans. A recent estimate of their global biomass was even a magnitude higher than the former estimate of approximately 1,000 million tons (Lam and Pauly 2005; Irigoien et al. 2014). Through extended diel vertical migrations (DVM) into shallower layers predominantly for feeding, the sheer biomass of mesopelagic fish has large influences on trophic connectivity and the carbon flux in the oceans (Saba et al. 2021). While the importance of pelagic fish communities for the nutrient flow in the oceans is widely acknowledged (e.g. Davison et al. 2013; Anderson et al. 2019; Saba et al. 2021), our understanding and knowledge of the vertical ecology of mesopelagic organisms in relation to their physico-chemical environment is still limited (St. John et al. 2016; Olivar et al. 2017; Proud et al. 2019; Romero-Romero et al. 2019) and studies on globally available data sets have demonstrated profound differences in the depth of day-time sound scattering layers between productive and oligotrophic regions (Bianchi and Mislan 2016; Klevjer et al. 2016).

From an oceanographic perspective, the Sargasso Sea is a particularly relevant transitional area in the western part of the North Atlantic. It is situated within the North Atlantic

L. Marohn and M. Schaber contributed equally to this work.

Communicated by S. E. Lluch-Cota

✉ L. Marohn
lasse.marohn@thuenen.de

[1] Thünen Institute of Fisheries Ecology, Herwigstr. 31, 27572 Bremerhaven, Germany

[2] Thünen Institute of Sea Fisheries, Herwigstr. 31, 27572 Bremerhaven, Germany

[3] Institute of Marine Ecosystem and Fishery Science, University of Hamburg, Große Elbstraße 133, 22767 Hamburg, Germany

Published online: 15 November 2021

Subtropical Gyre and surrounded by ocean currents, which can trap the water in the core of the Sargasso Sea for decades (Maximenko et al. 2012). This large marine ecoregion is influenced by various hydrographical features, including complex patterns of thermal fronts, mesoscale eddies, advective transport of water masses and seasonal convective overturn, which all have an influence on the biota and lead to a pronounced spatio-temporal variability in planktonic productivity (McGillicuddy et al. 1998; Hansell and Carlson 2001; Palter et al. 2005; Eden et al. 2009; Hellenbrecht et al. 2019). Based on the prevailing low nutrient levels, the Sargasso Sea is generally classified as oligotrophic. However, in spite of this fact, it has a high net primary production rate per unit area (Steinberg et al. 2001; Laffoley et al. 2011).

Besides environmental factors like primary production, oxygen concentration and light intensity (Irigoien et al. 2014; Klevjer et al. 2016; Aksnes et al. 2017), the distribution of pelagic fish in the Sargasso Sea may also be influenced by distinct temperature fronts in the upper 150 m of the ocean. These fronts may form zoogeographic boundaries for certain mesopelagic fish (Backus et al. 1969) and cephalopod species (Lischka et al. 2017) caused by temperature-related changes in e.g. productivity or stratification. Changes in mesopelagic fish species composition across fronts have been reported, for example at frontal systems in the southern California Current region, demonstrating incongruent patterns in the spatial distribution of migrators and non-migrators (Netburn and Koslow 2018). In the Sargasso Sea, these fronts are caused by the confluence of warm and cold-water masses in the subtropical convergence zone (STCZ) (Katz 1969). It has also been demonstrated that distribution and transport of midwater fish species can be driven by eddies (Olson and Backus 1985; Godø et al. 2012) including also the transport into or out of the Sargasso Sea (Craddock et al. 1992).

A large number of studies describe vertical distribution patterns of mesopelagic fish (e.g. Sutton 2013; Klevjer et al. 2016; Olivar et al. 2016; Proud et al. 2017; Sutton et al. 2017). The distribution of mesopelagic fish species in deep scattering layers (DSL) and the species composition of those layers have been identified on a regional scale in the temperate northeastern Atlantic and in the subtropical and tropical western Atlantic and adjacent waters (Roe and Badcock 1984; Wienerroither et al. 2009; Peña et al. 2014; Ariza et al. 2016; D'Elia et al. 2016). Abundance and distribution of mesopelagic fish have also been investigated in the Sargasso Sea (Backus et al. 1969; Backus et al. 1970; Jahn and Backus 1976; Backus and Craddock 1977; Gartner Jr et al. 1989; Sutton et al. 2010; Ayala et al. 2016). However, as for most ocean areas, current data on mesopelagics from this remote region are scarce.

To further increase our knowledge about the distribution and abundance of mesopelagic fish species in the Sargasso Sea, a hydroacoustic analysis of scattering layers and a series of depth stratified mesopelagic trawl samplings were conducted during an extensive multipurpose pelagic fishery survey along the subtropical convergence zone from 52° W to 70° W. Stratified catches were compared with hydroacoustic data, in order to assess the vertical migration behaviour of mesopelagic fish and to characterize the composition of deep scattering layer, providing insights into the horizontal and vertical distribution of fish species over this large oceanic area.

Material and methods

Fishing gear and sampling methodology

Sampling took place from March 20 to April 6, 2014, during an extensive multipurpose fishery survey (WH373) on the German R/V Walther Herwig III in the Sargasso Sea with a pelagic trawl (Engel Netze, Bremerhaven, Germany). The net had an opening width of 30 m, a height of 20 m, a length of 145 m, and mesh sizes (knot to knot) from 90 cm decreasing stepwise to 40, 20, 10, 5, 4, 3, 2 cm, with a 1.5 cm mesh in the 27 m long codend. It was equipped with a multi-closing system that enabled fishing in three defined depth strata by a time-controlled closing mechanism (multisampler).

Seven stations between 25°30′ and 29°30′ N and 52°00′ and 70°00′ W were sampled (Table 1, Fig. 1). Five stations (228, 240, 259, 284, 300, hereafter *regular stations*) were fished at night (starting time between 22:44 and 00:57 local time) at depths between ca. 150 and 370 m (Table 1). In addition, two deep hauls sampled the main scattering layers as observed by hydroacoustics (stations 233 and 316, hereafter *deep stations*): one during day-time (station 233: depth 108–698 m, 06:47–11:47 local time), and one during night-time (station 316: depth 31–965 m, 23:25–03:50) (Table 1).

Trawl duration at all stations was 225 min, with each of the 3 nets open for 75 min, apart from station 233, where net 1 was opened for 90 min and nets 2 and 3 for 105 min each (Table 1). All hauls were towed obliquely from shallower to deeper layers. Towing speed through water was 3 knots at all stations. The multisampler codends were cleaned from remaining fish after each haul.

Hydroacoustic data

Hydroacoustic data were collected continuously with a Simrad EK60 scientific echosounder operated at 18, 38, 120 and 200 kHz with hull-mounted transducers at a ship speed of approximately 12 knots during transit and 3 knots during fishing operations. Only data from the 18 kHz and 38 kHz transducer were used for further analyses. Beam widths of the transducers were 11° (18 kHz) and 7° (38 kHz), respectively, and both were operated at 2000 W. The pulse length was 1.024 ms with the ping rate set to maximum. To account for

Table 1 Sampling stations

Station	Date	Start position		Depth	Time		Time (local)		Duration
Net		lat (°N)	lon (°W)	(m)	Start (hrs:min) after sunset	End (hrs:min) before sunrise	Start	End	(min)
228	20.03.2014	27°30′	69°59′	152–346	05:03	02:44	22:54	02:59	225
net 1				152–208	05:03	05:34	22:54	00:09	75
net 2				225–275	06:28	04:09	00:19	01:34	75
net 3				293–346	07:53	02:44	01:44	02:59	75
240	23.03.2014	27°30′	66°59′	146–350	05:13	02:28	23:54	03:59	225
net 1				146–205	05:13	05:18	23:54	01:09	75
net 2				225–271	06:38	03:53	01:19	02:34	75
net 3				298–350	08:03	02:28	02:44	03:59	75
259	26.03.2014	25°33′	63°55′	157–356	06:27	01:10	00:57	05:02	225
net 1				157–208	06:27	04:00	00:57	02:12	75
net 2				220–277	07:52	02:35	02:22	03:37	75
net 3				265–356	09:17	01:10	03:47	05:02	75
284	30.03.2014	29°29′	60°59′	145–368	05:20	02:09	23:41	03:46	225
net 1				145–196	05:20	04:59	23:41	00:56	75
net 2				220–278	06:45	03:34	01:06	02:21	75
net 3				288–368	08:10	02:09	02:31	03:46	75
300	02.04.2014	26°29′	57°59′	150–342	04:35	02:52	22:44	02:49	225
net 1				150–230	04:35	05:42	22:44	23:59	75
net 2				225–265	06:00	04:17	00:09	01:24	75
net 3				295–342	07:25	02:52	01:34	02:49	75
233	21.03.2014	26°34′	69°59′	108–698	na	na	06:47	11:47	300
net 1				108–362	na	na	06:47	08:17	90
net 2				362–450	na	na	08:17	10:02	105
net 3				450–698	na	na	10:02	11:47	105
316	06.04.2014	27°02′	51°58′	32–965	04:37	02:22	23:25	03:50	225
net 1				32–152	04:37	05:32	23:25	00:40	75
net 2				482–606	06:17	03:52	01:05	02:20	75
net 3				774–965	07:47	02:22	02:35	03:50	75

surface turbulence and the transducer near-field, acoustic data were collected from 15 m below the surface down to 1000 m. The echosounder could not be calibrated prior, during or after survey operations, but had been calibrated on a dedicated hydroacoustic survey a few months prior with the standard sphere method (Foote et al. 1987; Demer et al. 2015). These

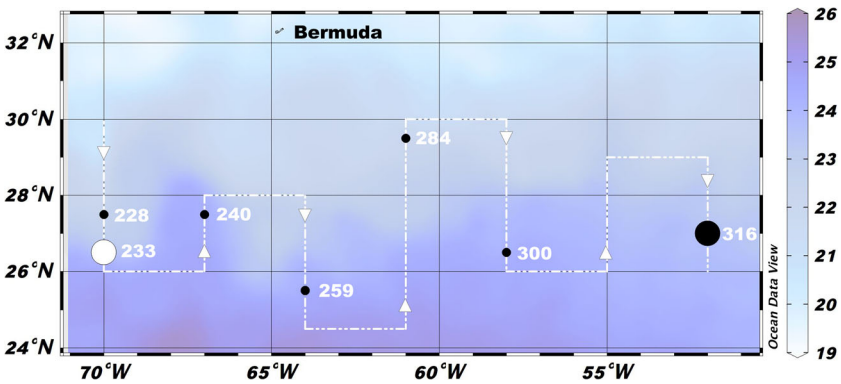

Fig. 1 Map of sampling stations. Colours represent sea surface temperature in °C on March 28 2014 (the mid-point of the sampling period). Small black circles represent *regular stations* and *deep stations* are presented by big circles (white=day-time, black=night-time). Cruise track and direction are represented by a dashed line and arrows

calibration results and parameters were used during data recording and post-processing, with ambient hydrographic parameters measured and implemented during recording based on CTD casts. Hydroacoustic data were post-processed using Echoview 12 software (Echoview Software Pty Ltd, Hobart, Australia). To mitigate signal degradation effects of noise and attenuation, different filters were applied to remove impulsive noise, transient noise and background noise (De Robertis and Higginbotto 2007; Ryan et al. 2015).

High backscattering values originate from targets with a density that differs strongly from the surrounding seawater that resonate when their dimensions are near the wavelength of a given frequency. Organisms with a density that is very similar to the surrounding medium produce a much weaker echo (Simmonds and MacLennan 2006). The former echoes mostly originate from organisms that bear a gas-filled structure, i.e. swimbladdered fishes, but also physonect siphonophores (Stanton et al. 1998; Korneliussen and Ona 2003; Proud et al. 2019), the latter from so-called fluid-like scatterers like cephalopods and crustaceans (Korneliussen and Ona 2003). Based on these backscattering characteristics, organisms that produce resonance at different incident frequencies can be classified.

A corresponding classification based on 18 and 38 kHz acoustic data was conducted. Acoustic backscatter was translated into volume backscattering (S_v, dB re 1 m^{-1}) and binned into cells of 2 min x 1 m depth for the duration of trawl sampling on each station and for 10 min x 10 m depth for a representative 72-h time-series of hydroacoustic data recorded on a transect section at 70° W illustrating several cycles of diel vertical migration. For each resulting cell, mean S_v was calculated at an integration threshold of −80 dB, and synthetic variable Δ_{Sv} was created by calculating S_v18-S_v38. This variable was used to identify functional groups of mesopelagic scatterers following a classification tree described by D'Elia et al. (2016). This classification is based on the size and scattering properties of different organism groups and allocates four categories to bins according to the following properties: small swimbladdered fishes (including small non-swimbladdered fishes and crustaceans; sm.(N)SB/Crust.) are $-14\ dB < \Delta_{Sv18kHz-38kHz} < -3\ dB$; large non-swimbladdered fishes (Lrg.NSB) are $-3\ dB < \Delta_{Sv18kHz-38kHz} < 0\ dB$; gelatinous zooplankton, cephalopods and pteropods, i.e. fluid-like scatterers (FL), are $0\ dB < \Delta_{Sv18kHz-38kHz} < 3\ dB$, and large swimbladdered fishes (Lrg.SB) are $3\ dB < \Delta_{Sv18kHz-38kHz} < 12\ dB$. Cells in which S_v was below the threshold (−80 dB, D'Elia et al. 2016) in either the 38 kHz or the 18 kHz data were classified as dominant Dom18 and Dom38, respectively. The corresponding acoustic scattering measured in both such cells can most likely be attributed to swimbladder-bearing fishes (Love 1978).

To evaluate the contribution of different taxonomic (fish) groups to the post-processed echograms, a classification of fishes according to the presence of a gas-filled (i.e. resonant) swimbladder was conducted and the corresponding families were categorized accordingly. A corresponding categorization was achieved using (identification) literature and swimbladder catalogues (Marshall 1960; Whitehead et al. 1986; Saenger 1989). Accordingly, the families Anoplogastridae, Bregmacerotidae, Chiasmodontidae, Gonostomatidae, Howellidae, Melamphaidae, Myctophidae, Phosichthyidae, Scombrolabracidae and Sternoptychidae were classified as fishes with swimbladder, whereas Evermannelidae, Notosudidae, Paralepididae and Stomiidae were classified as fishes without swimbladder. Species for which no information could be gathered were categorized into "other fish". Ontogenetic changes in swimbladder-structure (i.e. gas-filled in juveniles and lipid-filled in adults) as occurring in some families/genera were not taken into account.

CTD and sea surface temperature satellite data

In situ hydrographic measurements were conducted with a SBE 9/11 conductivity-temperature-depth probe (CTD) (Sea-Bird Electronic, Bellevue, WA, USA). CTD casts were made at all stations (depth 300–1000 m), recording conductivity, temperature, salinity and pressure (depth).

Prominent temperature fronts along the STCZ in the study area were observed via sea surface temperature (SST) data. SST data were derived from the Operational Sea Surface Temperature and Sea Ice Analysis (OSTIA) system (https://opendap.jpl.nasa.gov/opendap/OceanTemperature/ghrsst/data/L4/GLOB/UKMO/OSTIA/2014/028/contents.html). Figure 1 depicts SST on March 28, 2014, as this date represents the mid-point of the sampling period.

Catch analysis and species identification

Total catches were sorted and divided into major taxonomic groups immediately after each haul and frozen at −20°C for transport and further utilization. After thawing, all fish specimens were identified to the lowest possible taxonomic level by the use of region-specific identification keys (Whitehead et al. 1986; FWNA 1989; Carpenter 2002; Richards 2005) and standard length and weight were assessed individually to the lowest 1.0 mm and rounded to the nearest 0.1 g, respectively. Regarding invertebrates, the analysis was limited to the assessment of total weight per group (mollusca, crustacea, gelatinous plankton) and haul.

Genetic analyses of subsamples of fish species were used to verify the morphological identification (for analytical methods see below). In case the results did not match with morphological species identification, morphological examination and identification were repeated and species names were revised or assigned to higher taxonomic ranks.

The influence of sea surface temperature on the abundance of the most dominant species was tested by a linear regression model (R Core Team 2019).

Genetic analysis

Tissue samples of representative individuals from each species or group were preserved in ethanol (96% abs.) for subsequent genetic analysis. DNA was extracted using Chelex100 (Walsh et al. 1991) and stored at +4°C or at −80°C for long-term storage. For DNA barcoding, the mitochondrial markers Cytochrome c oxidase I (COI) and Cytochrome b (Cytb) and the nuclear marker Myosin heavy chain 6 (myh6) were amplified by polymerase chain reactions (PCR). All PCRs were carried out using High-Fidelity PCR Master Mix with HF Buffer (Phusion, New England Biolabs), 0.25 μM of each primer (Table 2), 3 μl template (using the supernatant of the Chelex extracted samples). Finally, nuclease-free water was added until a final volume of 20 μl was reached. Amplification was accomplished with a T3 Thermocycler (Biometra/Analytik Jena, Germany) with the following cycling conditions: initial denaturation at 98°C for 30 s, followed by 32 cycles for COI and 35 cycles for Cytb, consisting of 98°C for 10 s, primer annealing for 30 s (COI at 53°C, Cytb at 51°C), extension at 72°C (COI for 20 s, Cytb for 40 s) and a final extension step at 72°C for 8 min. For myh6 amplification, a special cycling protocol was used with the following conditions: initial denaturation at 98°C for 30 s, followed by a primer annealing touchdown step with 8 cycles, consisting of 98°C for 10 s, primer annealing decreasing with 1°C from 62°C to 54°C in each cycle for 30 s, extension at 72°C for 30 s, followed by 30 cycles with 98°C for 10 s, 54°C for 30 s, 72°C for 30 s and final extension at 72°C for 7 min. As a quality check, 5 μl of each PCR product was analysed with standard agarose gel electrophoresis (1% agarose, stained with ethidium bromide). PCR products showing strong sharp and clear bands with the right amplicon size were diluted with ultra-pure water. Products showing weak bands were purified and concentrated using PCR and DNA Cleanup Kits (Monarch, New England Biolabs, T1030) prior to sequencing. Sequence raw data were checked and edited with CodonCode Aligner Software (Centerville MA, USA) by cutting off primer sites and generating consensus sequences. To verify the results of the morphological identification, all obtained sequences were compared with NCBIs Nucleotide Sequence Database by BLAST (Altschul et al. 1990).

Results

Hydrography

Depth profiles of temperature and salinity varied among sampling stations (Fig. 2). A well-defined thermocline was present at all stations between 100 and 200 m depth. Sea surface temperatures varied between 22.5 and 24.9°C, with the lowest temperatures being measured at northern-, western- and easternmost stations (stations 284, 228 and 316) (Fig. 1). Within the upper 200 m, temperatures dropped at about 4–5°C to 18.5–20.7°C and at 500 m depth temperatures between 15.5 and 17.2°C were measured. Trawls at *regular stations* took place in depths with temperatures between 18 and 22°C, while *deep stations* reached temperatures below 7°C at greater depths. Sea surface temperature data showed a distinct temperature front between 24° N and 30° N in the western part of the study area, with temperatures decreasing northwards from above 25°C to below 22°C (Fig. 1). In the eastern part of the study area, the front was less pronounced.

Water salinity decreased vertically from around 36.5 near the surface to 35 at 1000 m depth. Within the upper 500 m, salinity values ranged from 36.1 to 37.2.

Table 2 List of primers for genetic analyses

Barcoding marker	Primer name	Primer sequence (5′-3′)
COI	VF2_t1_M13	TGTAAAACGACGGCCAGTCAACCAACCACAAAGACATTGGCAC
	FishF2_t1_M13	TGTAAAACGACGGCCAGTCGACTAATCATAAAGATATCGGCAC
	FishR2_t1_M13	CAGGAAACAGCTATGACACTTCAGGGTGACCGAAGAATCAGAA
	FR1d_t1_M13	CAGGAAACAGCTATGACACCTCAGGGTGTCCGAARAAYCARAA
	Ivanova et al. 2007 (modified with M13 sequencing sites)	
Cytb	FishcytB-F_M13F	TGTAAAACGACGGCCAGTACCACCGTTGTTATTCAACTACAAGAAC
	TruccytB-R _M13R	CAGGAAACAGCTATGACCCGACTTCCGGATTACAAGACCG
	Sevilla et al. 2007 (modified with M13 sequencing sites)	
Myh6	myh6_F507_M13	TGTAAAACGACGGCCAGTGGAGAATCARTCKGTGCTCATCA
	myh6_R1322_M13	CAGGAAACAGCTATGACCCTCACCACCATCCAGTTGAACAT
	Li et al. 2007 (modified with M13 sequencing sites)	

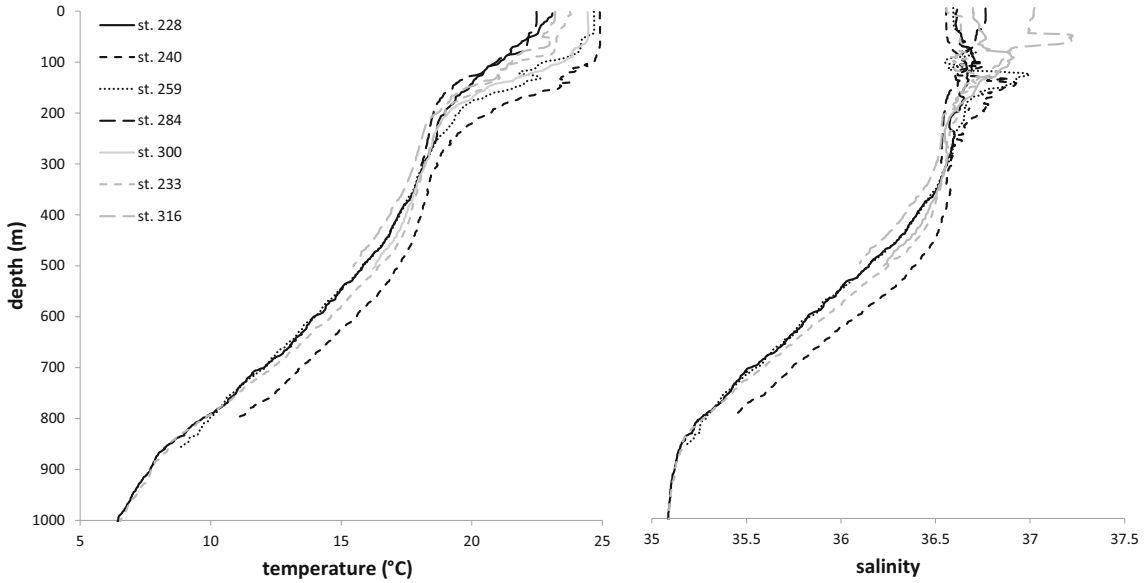

Fig. 2 Temperature and salinity depth profiles at sampling stations

Hydroacoustics: general mesopelagic habitat structure

From hydroacoustic data, a common pattern of scattering layers was evident throughout the survey area and along the sampled transects, with persistent stationary and several migrating components of different scattering characteristics (Figs. 3, 4 and 5). In the epipelagic zone, dense stationary echoes were visible especially in the upper 150 m of the water column (epipelagic layer, hereafter referred to as layer 1). In the mesopelagic zone, two separate deep scattering layers (DSLs) were evident: one dense layer was most prominent in the 18 kHz echodata between 450 and 600 m (Figs. 3, 4 and 5b) and between 400 and 700 m in the 38 kHz data (upper mesopelagic scattering layer, hereafter referred to as principal DSL and layer 2). A weaker scattering layer around 800–900 m depth was most prominent in the 18 kHz data (Figs. 3, 4 and 5a) (lower mesopelagic scattering layer, hereafter referred to as secondary DSL and layer 3). Based on the classification of acoustic data through Δ_{Sv}, layer 1 contained echoes originating from a variety of organisms, namely swimbladdered as well as non-swimbladdered fishes, fluid-like scatterers and crustaceans — with varying contributions during day- and night-time. The upper part of the principal DSL (layer 2) (400–500 m) consisted mostly of (large) swimbladdered and non-swimbladdered fishes with clear contributions of fluid-like scatterers, while the deeper parts of the principal DSL (layer 2) (500–700 m) were dominated by small swimbladdered and non-swimbladdered fishes and crustaceans (Figs. 3, 4 and 5c).

From the echograms recorded at either frequency, a clear and regular diel pattern was evident with different components emerging from both DSLs at different times and undertaking diel vertical migration (Fig. 3).

Beginning from ca. 16:00 h local time (ca. 2 h before sunset), an upward migrating layer emerged from the principal DSL (layer 2) and by 19:00 h merged with layer 1. A second cohort of organisms undertaking DVM emerged from the deeper secondary DSL (layer 3) around 17:00 h. This group ascended through the principal DSL (layer 2) and merged during its ascent with the previous cohort from this layer shortly before merging with layer 1. The migrating components appeared to mostly consist of swimbladdered and non-swimbladdered fishes as well as fluid-like scatterers. For the next ca. 9 h, layer 1 appeared both denser (in terms of acoustic backscatter) and of different composition (through the contribution of the migrating components). While during day-time the epipelagic layers seemed to be mostly dominated by small swimbladdered and non-swimbladdered fishes and crustaceans, distinct additional contributions of fluid-like scatterers as well as large swimbladdered and non-swimbladdered fishes were evident during night (Fig. 3c). Starting from ca. 04:00 h, several descending layers became evident leaving layer 1 and the epipelagic zone, with the components from the secondary DSL (layer 3) showing a faster descent into that depth than the components of the principal DSL (layer 2). By ca. 07:00 h, the faster descending migrating component of layer 3 merged into that layer again, while the migrating organisms from layer 2 merged into the stationary component ca. 1 h later.

Depth distribution of mesopelagic fish and taxonomic composition of scattering layers

Regular stations

Night-time multisampler hauls in depths between ca. 150 and ca. 360 m at stations 228, 240, 259, 284 and 300 were

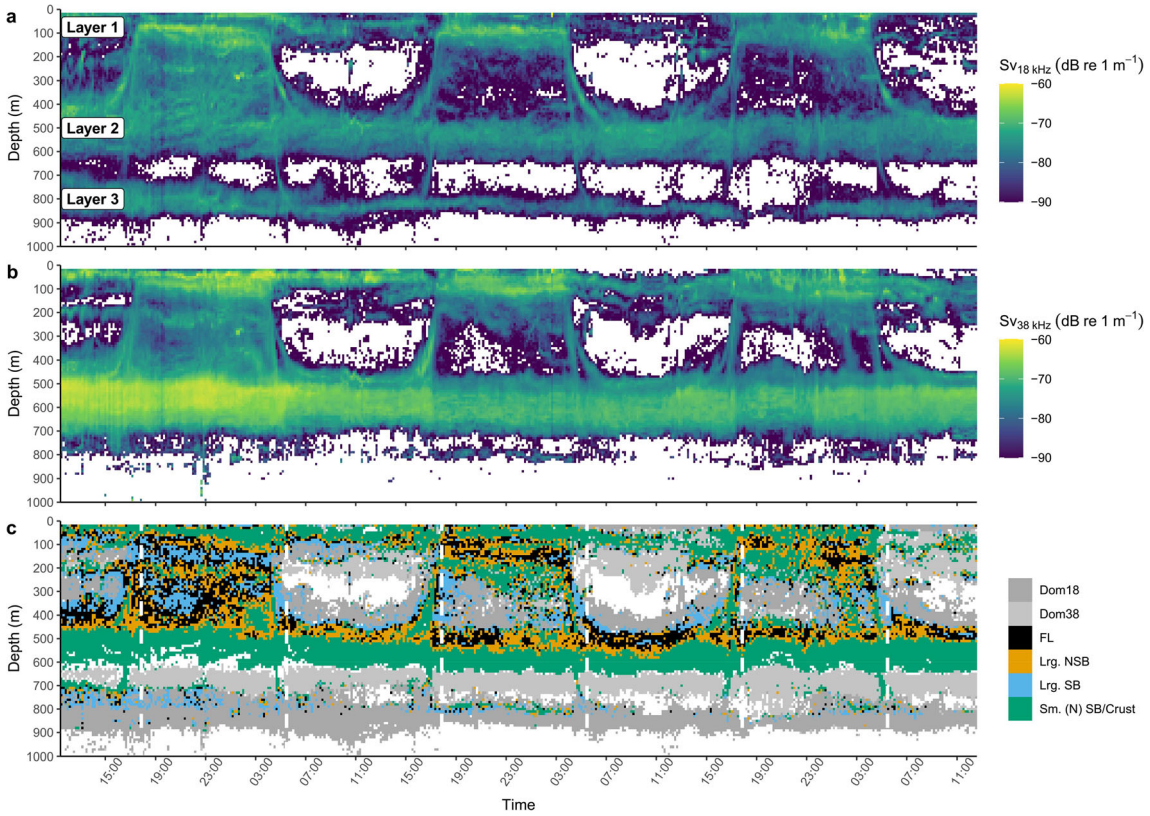

Fig. 3 Example of hydroacoustic data recorded along a 72-h period on the latitudinal transect following 70° W showing three cycles of diel vertical migration. Scattering layers as investigated and referred to in the main text are indicated in panel **a** (layer 1 — epipelagic layer; layer 2 — principal DSL; layer 3 — secondary DSL). **a** Volume backscattering Sv recorded at 18 kHz; **b** Sv recorded at 38 kHz; **c** classification of hydroacoustic data based on Δ_{Sv} (S_v18-S_v38) (D´Elia et al. 2016): FL, fluid-like scatterers (gelatinous zooplankton, cephalopods and pteropods); Lrg. NSB, large non-swimbladdered fishes; Lrg. SB, large swimbladdered fishes; sm. (N)SB/Crust., small swimbladdered fishes (including small non-swimbladdered fishes and crustaceans). Cells in which S_v was below the threshold in either the 38 kHz or the 18 kHz data were classified as dominant Dom18 and Dom38, respectively. The corresponding acoustic scattering measured in both such cells can most likely be attributed to swimbladder-bearing fishes (Love 1978). White, dashed vertical lines indicate sunset and sunrise, respectively

conducted with uniform trawl paths and depth profiles. There, the upper net 1 (ca. 150–220 m) partly covered the dense epipelagic layer (layer 1) that appeared during night-time after migrating organisms had completed their DVM. Layer 1 was classified as most likely consisting of a mixture of components, with contributions of swimbladdered, non-swimbladdered and fluid-like scatterers. Nets 2 (ca. 220–280 m) and 3 (ca. 280–360 m) covered depths below layer 1, in which echoes were less dense and most likely originated from resonant, swimbladdered fish and, to a lesser extent, of fluid-like scatterers (Fig. 4c). In all depth layers covered by the multisampler tows, swimbladdered fish species dominated the catches by total catch weight, and fishes without a swimbladder only marginally contributed to the bulk catch across all depth layers (Fig. 6). In these night-time catches, Myctophidae dominated especially the shallowest samples taken from layer 1 (net 1), while their number decreased in deeper samples (nets 2 and 3) (Table 3). The second most dominant family was Melamphaidae, with highest numbers in net 2 and lowest numbers in the deepest samples. Other important families that contributed to the catch in all sampled layers, albeit in distinctly lower numbers, were Gonostomatidae (all *Sigmops elongatus*), Stomiidae, Scombrolabracidae (all *Scombrolabrax heterolepis*) and Evermannellidae (mostly *Coccorella atlantica*). In all but the Gonostomatidae (i.e. *S. elongatus)*, numbers were highest in shallower samples (nets 1 and 2). The latter occurred in higher numbers in the deeper tows (nets 2 and 3). Sternoptychidae were only sampled in the deeper layers (nets 2 and 3) with highest numbers in the deepest tows. Other fish families were caught in distinctly lower numbers.

No clear trend was evident in the fractions of other organisms across hauls. The second most important organism group were molluscs (mostly cephalopods). In general, molluscs contributed stronger to the total catch weight of the shallowest net than of the deeper nets and they are assumed to contribute to the fluid-like backscatter measured in these depths. Crustaceans were also present in all hauls with similar fractions across all sampled depth layers (Fig. 6). Gelatinous zooplankton only marginally contributed to the catches.

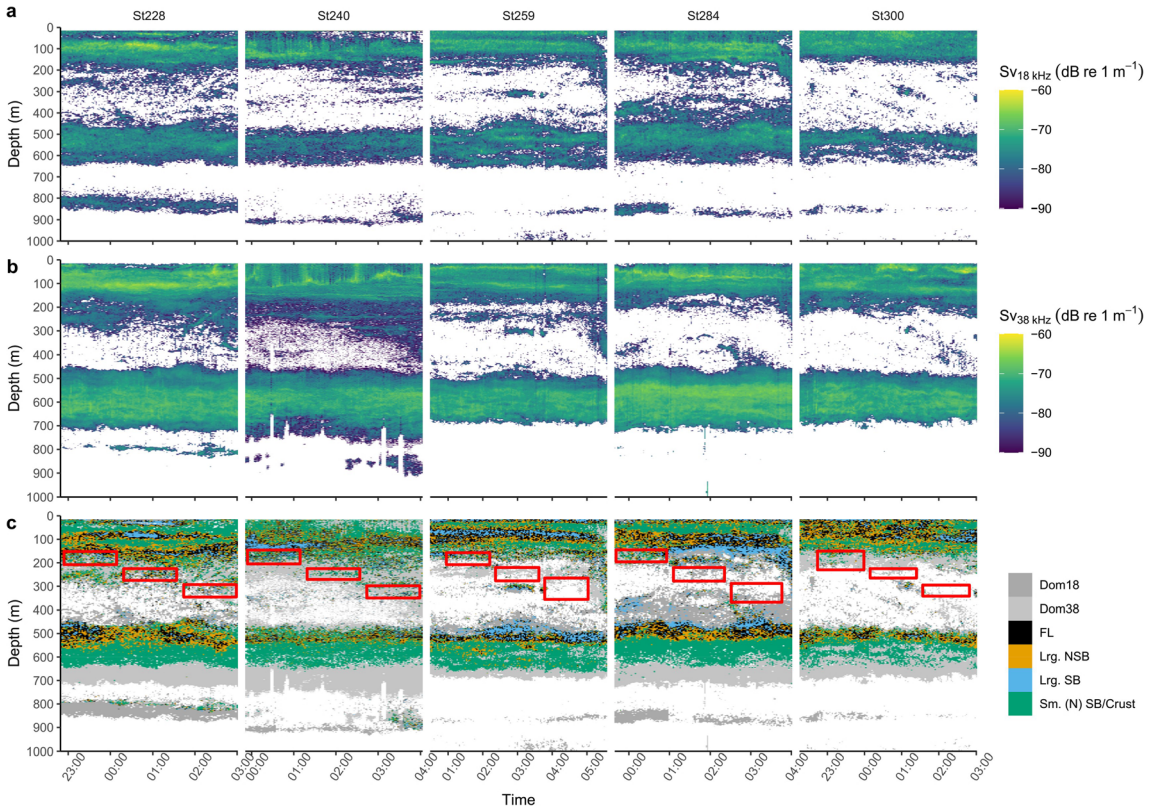

Fig. 4 Hydroacoustic data recorded at *regular stations*. **a** Volume backscattering Sv recorded at 18 kHz; **b** Sv recorded at 38 kHz; **c** classification of hydroacoustic data based on Δ_{Sv} (S_v18-S_v38) (D´Elia et al. 2016): FL, fluid-like scatterers (gelatinous zooplankton, cephalopods and pteropods); Lrg. NSB, large non-swimbladdered fishes; Lrg. SB, large swimbladdered fishes; sm. (N)SB/Crust., small swimbladdered fishes (including small non-swimbladdered fishes and crustaceans). Cells in which S_v was below the threshold in either the 38 kHz or the 18 kHz data were classified as dominant Dom18 and Dom38, respectively. The corresponding acoustic scattering measured in both such cells can most likely be attributed to swimbladder-bearing fishes (Love 1978). For each station, trawl paths, i.e. regions and layers covered by the three nets of the multisampler, are indicated by red rectangles in panel **c**

Deep stations

On the deep day-time station (233), located at the western part of the study area, an increase in total catch (abundance and biomass) was evident with increasing depth and a dominance of different organism groups in terms of catch weight became evident (Table 4). Samples collected at that station were taken in depths covering the layers 1 (net 1, 108–362 m) and 2 (net 2, 362–450 m and net 3, 450–698 m). Net 1 was dominated by molluscs (ca. 60% of catch weight), followed by crustaceans and swimbladdered fishes (both ca. 20% of catch weight) (Fig. 6). According to the scattering properties described above, this depth contained swimbladdered fishes as well as fluid-like scatterers and contributions of small swimbladdered and non-swimbladdered fishes and crustanceans (Fig. 5c). Net 2, i.e. samples from the upper part of layer 2, was dominated by gelatinous zooplankton (ca. 50% of catch weight), followed by swimbladdered fishes (ca. 30% of catch weight) and crustaceans (ca. 20% of catch weight). Corresponding echo signals were classified as consisting mainly of swimbladdered fishes and fluid-like scatterers (Fig. 5c). Net 3, the main part of layer 2, showed a similar catch composition, with gelatinous zooplankton contributing ca. 75% to the catch weight, swimbladdered fishes accounting for ca. 20% and crustaceans for ca. 5%. The depth range covered by net 3 was dominated by the acoustic classes of small swimbladdered and non-swimbladdered fishes and crustaceans (Fig. 5c).

Myctophidae, followed by Gonostomatidae, was the most important fish family caught at that station. The bulk of specimens was caught in the deepest net 3 sampling layer 2 (ca. 450–700 m), with distinctly lower numbers in net 2 and lowest numbers in net 1. Gonostomatidae were absent from the shallower nets 1 and 2.

The deep night-time station (316) was located approximately 1,790 km further east from the deep day-time station (233) and covered the water column down to 965 m. At this station, layer 1 (net 1, 32–152 m) and the upper part of layer 2 (net 2, 482–606 m) as well as layer 3 (net 3, 775–965 m) were sampled (Fig. 5c) and a decrease in the number of individuals became evident with increasing depth. Catches in terms of weight were dominated by swimbladdered fishes in the shallowest net (net 1, ca. 85%) with small contributions of gelatinous zooplankton and molluscs (ca. 6% each) and

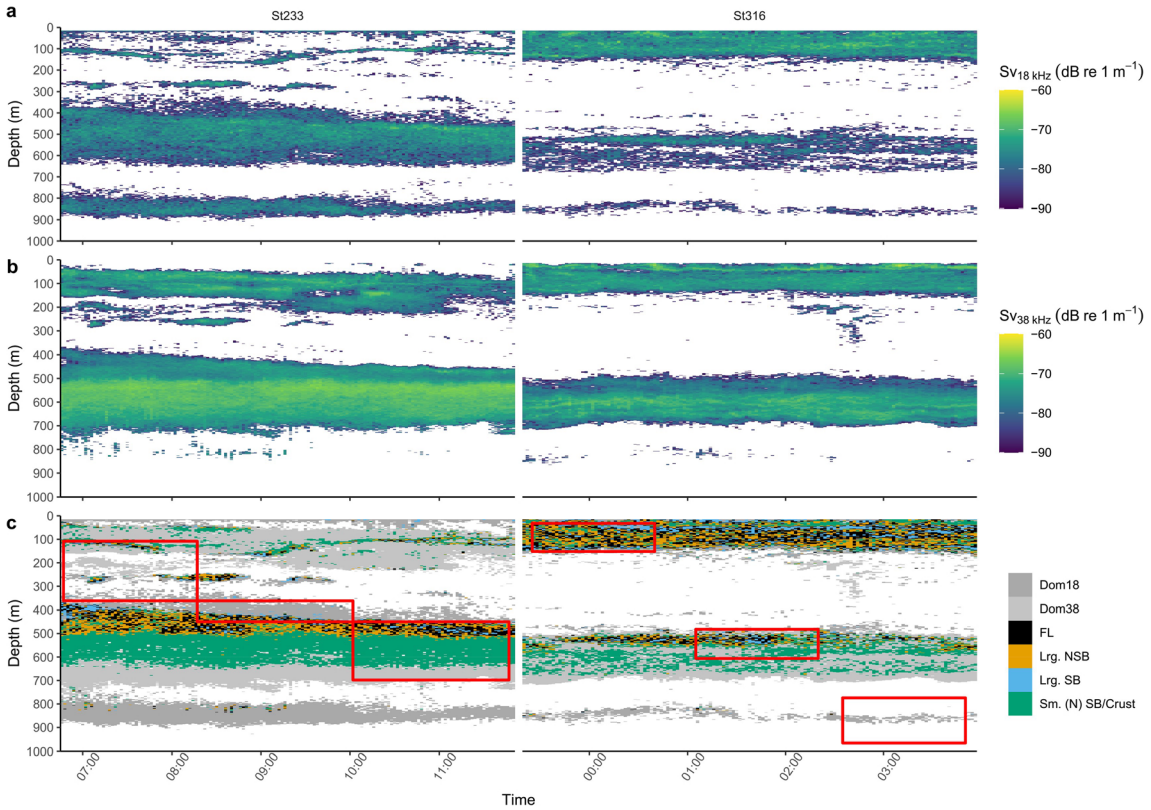

Fig. 5 Hydroacoustic data recorded at *deep stations*. St. 233 (left panels) was sampled during day-time, St. 316 (right panels) was sampled at night. **a** Volume backscattering Sv recorded at 18 kHz; **b** Sv recorded at 38 kHz; **c** classification of hydroacoustic data based on Δ_{Sv} (S_v18-S_v38) (D´Elia et al. 2016): FL, fluid-like scatterers (gelatinous zooplankton, cephalopods and pteropods); Lrg. NSB, large non-swimbladdered fishes; Lrg. SB, large swimbladdered fishes; sm. (N)SB/Crust., small swimbladdered fishes (including small non-swimbladdered fishes and crustaceans). Cells in which S_v was below the threshold in either the 38 kHz or the 18 kHz data were classified as dominant Dom18 and Dom38, respectively. The corresponding acoustic scattering measured in both such cells can most likely be attributed to swimbladder-bearing fishes (Love 1978). For each station, trawl paths, i.e. regions and layers covered by the three nets of the multisampler, are indicated by red rectangles in panel **c**

negligible fractions of crustaceans. A mixture of the corresponding categories had also been allocated to the hydroacoustic data collected from this layer. Fishes collected with that net were almost exclusively Myctophidae, with Phosichthyidae and Melamphaidae only marginally contributing to the catch (Table 4). Catches from net 2, sampling layer 2, were also dominated by fishes, with fishes without a swimmbladder constituting the bulk (50%) and fishes with a swimbladder and uncategorized fishes contributing smaller fractions (17 and 11%, respectively) (Fig. 6). Crustaceans contributed with 15%, while gelatinous zooplankton and molluscs each contributed with less than 5% to the total catch weight. Among fishes, Melamphaidae, Myctophidae and Gonostomatidae were dominant, albeit in far lower numbers than in the upper 150 m (Table 4). Other families, such as Evermannellidae, Stomiidae, Chiasmodontidae and Sternoptychidae, also contributed to the catch with several individuals of each family. In the deepest net (net 3), gelatinous zooplankton was the dominant fraction (40%), followed by crustaceans (20%) and fish (swimbladdered, no swimbladder and others with 19, 14 and 4%, respectively). Fish families sampled at that depth were mostly Stomiidae, Myctophidae, Gonostomatidae and Sternoptychidae (Table 4). Species that were caught exclusively at depth below 360 m were *Bonapartia pedaliota* (*N*=67), *Cyclothone* spec. (*N*=9), *Serrivomer beanii* (*N*=4) and *Poromitra crassiceps* (*N*=1).

Taxonomic and quantitative fish catch composition

The total catch consisted of 5022 fish specimens from 27 families, 62 genera and 70 species of which 4050 individuals (80.7%) were identified to species level, 813 (16.2%) to genus level, and 137 (2.7%) to family level. Twenty-two specimens (0.4%) remained entirely unidentified due to mechanical damages in the net during trawling. An overview of the total catch at stations and depths is presented in Table 5, detailed information about catch composition is given in Table 6, and length and weight data as well as results from genetic analyses are presented in Table 7.

In terms of abundance (N), relative abundance (A) and biomass (M), the total fish catch was dominated by Myctophidae (N=2970, A=59.1%, M=47.4% of total catch),

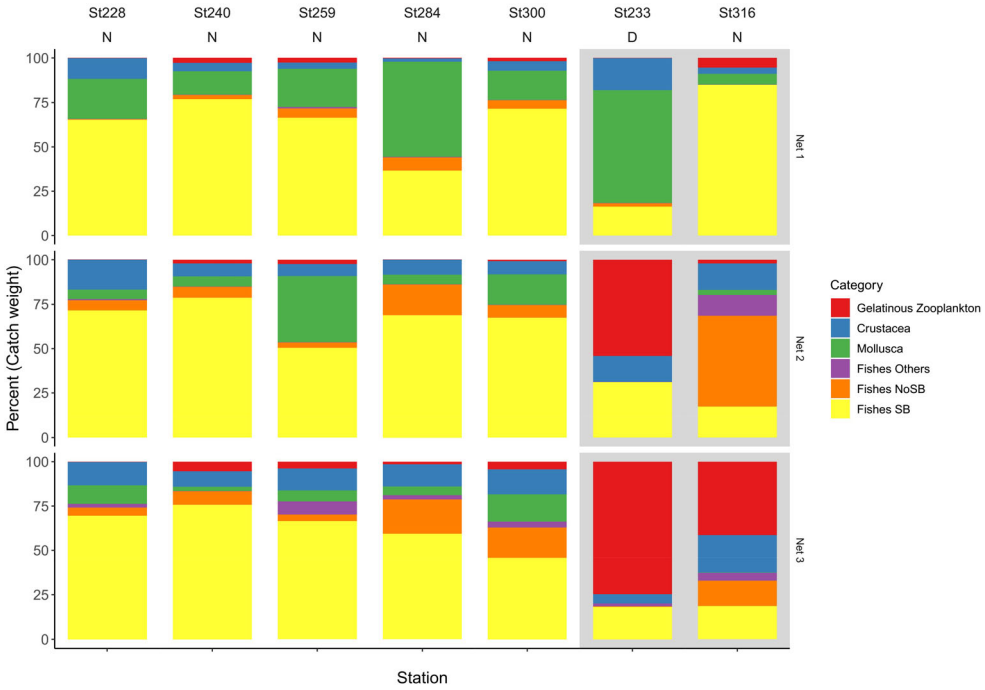

Fig. 6 Catch composition (percentage of total catch weight per net) of major taxonomic categories in different depth strata covered during *regular* and *deep* night- (N) and day-time (D) stations. *Regular stations*: net 1 (upper panel): 150–220 m; net 2 (middle panel): 220–280 m; net 3 (lower panel): 280–350 m. *Deep stations* (panels with grey background). Station 233: net 1: 100–350 m; net 2: 350–450 m; net 3: 450–700 m. Station 316: net 1: 30–150 m; net 2: 480–600 m; net 3: 775–965 m. NOSB, without swimbladder; SB, with swimbladder

Melamphaidae (N=1192, A=22.5%, M=17.1%), Gonostomatidae (N=225, A=4.5%, M=11.3%), Stomiidae (N=106, A=2.1%, M=8.5%) and Sternoptychidae (N=81, A=1.6%, M=2.9%). Four species accounted for 50.3% of the total number of fishes: the melamphaid *Scopelogadus mizolepis* was the most abundant species (N=962,

Table 3 Total number of caught specimen (N), relative abundance (A), total catch weight and relative biomass (M) of fish families at depth (*regular stations* 228, 240, 259, 284 and 300). The table includes all families that contain more than 5 specimens

Family	Net 1 (ca. 150-220 m)				Net 2 (ca. 220–280 m)				Net 3 (280–360 m)			
	Number (N)	A (%)	Weight (kg)	M (%)	Number (N)	A (%)	Weight (kg)	M (%)	Number (N)	A (%)	Weight (kg)	M (%)
Myctophidae	1511	69.2	2.972	74.4	348	32.9	0.737	27.8	304	39.3	0.740	27.5
Melamphaidae	407	18.6	0.431	10.8	494	46.6	0.871	32.9	268	34.7	0.542	20.1
Gonostomatidae	32	1.5	0.083	2.1	63	5.9	0.419	15.8	53	6.9	0.650	24.1
Stomiidae	43	2.0	0.186	4.7	23	2.2	0.164	6.2	17	2.2	0.239	8.9
Scombrolabracidae	35	1.6	0.070	1.8	31	2.9	0.116	4.4	3	0.4	0.007	0.2
Sternoptychidae	0	n.a.	n.a.	n.a.	15	1.4	0.053	2.0	48	6.2	0.226	8.4
Evermannellidae	21	1.0	0.053	1.3	24	2.3	0.092	3.5	16	2.1	0.068	2.5
Anoplogastridae	5	0.2	0.003	0.1	13	1.2	0.013	0.5	19	2.5	0.019	0.7
Bregmacerotidae	30	1.4	0.060	1.5	3	0.3	0.011	0.4	2	0.3	0.007	0.3
Howellidae	15	0.7	0.032	0.8	11	1.0	0.055	2.1	3	0.4	0.020	0.7
Notosudidae	19	0.9	0.058	1.5	6	0.6	0.032	1.2	2	0.3	0.014	0.5
Chiasmodontidae	4	0.2	0.003	0.1	12	1.1	0.072	2.7	10	1.3	0.049	1.8
Paralepididae	16	0.7	0.023	0.6	6	0.6	0.010	0.4	1	0.1	0.005	0.2
Phosichthyidae	11	0.5	0.002	0.0	1	0.1	0.001	0.0	8	1.0	0.001	0.0
Tetraodontidae	13	0.6	0.001	0.0	0	n.a.	n.a.	n.a.	0	0.0	n.a.	n.a.
Scopelarchidae	0	n.a.	n.a.	n.a.	2	0.2	0.0002	0.0	9	1.2	0.0214	0.8
Bramidae	9	0.4	0.008	0.2	0	n.a.	n.a.	n.a.	0	n.a.	n.a.	n.a.
Trichiuridae	5	0.2	0.002	0.1	1	0.1	0.003	0.1	1	0.1	0.045	1.7
Molidae	5	0.2	0.0004	0.0	0	n.a.	0.737	n.a.	1	0.1	0.0001	0.0

Table 4 Total number of caught specimens and total weight of fish per family at *deep stations* (233 and 316)

Family	Station 233					
	Net 1 (108–362 m)		Net 2 (362–450 m)		Net 3 (450–698 m)	
	Number (N)	Weight (kg)	Number (N)	Weight (kg)	Number (N)	Weight (kg)
Myctophidae	4	0.008	5	0.005	77	0.077
Gonostomatidae	n.a.	n.a.	n.a.	n.a.	57	0.057
Phosichthyidae	n.a.	n.a.	10	0.01	n.a.	n.a.
Sternoptychidae	1	0.0002	7	0.007	3	0.003
Stomiidae	n.a.	n.a.	n.a.	n.a.	6	0.006
Melamphaidae	n.a.	n.a.	2	0.002	1	n.a.
Howellidae	n.a.	n.a.	2	0.002	2	0.002
Diretmidae	n.a.	n.a.	n.a.	n.a.	2	0.002
Molidae	n.a.	n.a.	n.a.	n.a.	2	n.a.
Paralepididae	1	0.001	n.a.	n.a.	n.a.	n.a.
Tetraodontidae	1	n.a.	n.a.	n.a.	n.a.	n.a.
Anoplogastridae	1	0.0004	n.a.	n.a.	n.a.	n.a.
Scopelarchidae	n.a.	n.a.	n.a.	n.a.	1	0.001
	Station 316					
	Net 1 (32–152 m)		Net 2 (482–606 m)		Net 3 (775–965 m)	
Myctophidae	698	0.617	12	0.021	11	0.02
Gonostomatidae	n.a.	n.a.	11	0.017	9	0.003
Phosichthyidae	4	0.001	19	0.034	1	0.018
Sternoptychidae	n.a.	n.a.	3	0.006	9	0.006
Stomiidae	n.a.	n.a.	3	0.201	13	0.149
Evermannellidae	n.a.	n.a.	6	0.069	n.a.	n.a.
Melamphaidae	2	n.a.	n.a.	n.a.	n.a.	n.a.
Chiasmodontidae	n.a.	n.a.	3	0.015	1	0.152
Serrivomidae	n.a.	n.a.	n.a.	n.a.	4	0.043
Diretmidae	n.a.	n.a.	n.a.	n.a.	1	0.002
Melanocetidae	n.a.	n.a.	1	0.062	n.a.	n.a.
Notosudidae	n.a.	n.a.	1	0.003	n.a.	n.a.

A=19.2%) followed by three myctophids (*Ceratoscopelus warmingii* (N=637, A=12.7%), *Nannobrachium* (*cf.*) *cuprarium* (N=612, A=12.2%) and *Bolinichthys photothorax* (N=309, A=6.2%)). Considerable numbers of *S. elongatus* (N=148, A=2.9%), *Lepidophanes guentheri* (N=148, A=2.9%), *Lampanyctus photonotus* (N=143, A=2.8%), *Lobianchia gemellari* (N=118, A=2.3%), *Lampadena atlantica* (N=104, A=2.1%) and *Diaphus mollis* (N=95, A=1.9%) were also recorded.

Table 5 Total number of caught specimens (N) and total catch weight per group at stations

Station	Depth	Fish		Mollusca	Crustacea	Gelat.
	(m)	(N)	(kg)	(kg)	(kg)	zoopl. (kg)
228	152–346	602	1.37	0.22	0.26	0.00
240	146–350	786	1.78	0.18	0.15	0.08
259	157–356	1083	2.24	0.78	0.23	0.09
284	145–368	839	2.36	1.28	0.21	0.02
300	150–342	706	1.58	0.35	0.16	0.04
233	108–698	194	0.31	0.04	0.09	1.00
316	32–965	812	1.44	0.06	0.33	0.49

The most species-rich families were Myctophidae (14 genera, 31 species) and Stomiidae (12 genera, 12 species) followed by Sternoptychidae and Phosichthyidae (3 genera, 4 species), and Melamphaidae, Evermannellidae, Gonostomatidae and Paralepididae (3 genera, 3 species). Genera with more than two species were *Diaphus* (10 species) and *Hygophum* (4) (both myctophids).

Genetic analysis of samples from 77 different species and groups of higher taxa were performed. In 58 cases, the morphologic identification was confirmed by genetic results. In 11 of these cases, specimens were assigned to higher taxonomic ranks, because morphologic and genetic identification did not match at species level (i.e. results did not match with sufficient

Table 6 Fish species per station and depth

Order Family Species		Regular stations															Deep stations					
		Station 228			Station 240			Station 259			Station 284			Station 300			Station 233			Station 316		
		Net 1	Net 2	Net 3	Net 1	Net 2	Net 3	Net 1	Net 2	Net 3	Net 1	Net 2	Net 3	Net 1	Net 2	Net 3	Net 1	Net 2	Net 3	Net 1	Net 2	Net 3
	Depth	152–	225–	293–	146–	225–	298–	157–	220–	265–	145–	220–	288–	150–	225–	295–	108–	362–	450–	32–	482–	774–
	(m)	208	275	346	205	271	350	208	277	356	196	278	368	230	265	342	362	450	698	152	505	965
	Time	22:54–	00:19–	01:44–	23:54–	01:19–	02:44–	00:57–	02:22–	03:47–	23:41–	01:06–	02:31–	22:44–	00:09–	01:34–	06:47–	08:17–	10:02–	23:25–	01:05–	02:35–
	(local)	00:09	01:34	02:59	01:09	02:34	03:59	02:12	03:37	05:02	00:56	02:21	03:46	23:59	01:24	02:49	08:17	10:02	11:47	00:40	02:20	03:50
	Total catch	Catch per net			Catch per net			Catch per net			Catch per net			Catch per net			Catch per net			Catch per net		
	N	N	N	N	N	N	N	N	N	N	N	N	N	N	N	N	N	N	N	N	N	N
Anguilliformes																						
Derichthyidae																						
Derichthys serpentinus	1						1															
Nemichthyidae																						
Nemichthys scolopaceus	1												1									
Serrivomeridae																						
Serrivomer beanii	4																					4
Serrivomeridae spec.	2						1									1						
Aulopiformes																						
Evermannellidae																						
Coccorella atlantica	63		8	4	1					1	18	14	1	1	2	7					6	
Evermannella indica	1												1									
Odontostomops normalops	1												1									
Evermannellidae spec.	2				1											1						
Notosudidae																						
Scopelosaurus smithii	26				2	1		10	2	1	1		1	5	2						1	
Scopelosaurus spec.	2	1	1																			
Paralepididae																						
Lestidiops spec.	17				3	3					5			5	1							
Macroparalepis brevis	1											1										
Sudis spec.	4			1	1				1								1					
Paralepididae spec.	2	2																				
Scopelarchidae																						
Scopelarchus analis	2									1									1			
Scopelarchus spec.	10		1	5		1										3						
Beryciformes																						
Anoplogastridae																						
Anoplogaster spec.	38		2	2	2	2	4	2	5	5	1	1	6		3	2	1					
Diretmidae																						
Diretmoides spec.	5		2																2			1
Gadiformes																						
Bregmacerotidae																						
Bregmaceros spec.	35	6	2	2	1			5			4	1		14								
Melanonidae																						
Melanonus zugmayeri	3			1						1	1											
Lophiiformes																						
Melanocetidae																						
Melanocetus johnsonii	1																				1	
Myctophiformes																						
Myctophidae																						
Bolinichthys indicus	22		2	1							1								4	14		
Bolinichthys photothorax	309	87	12	9	24	3	6	81	28	17	7	1	1	26	3	3				1		
Bolinichthys spec.	3				1							1										1
Ceratoscopelus warmingii	638	22	2	2	90	14	51	78	24	29	21	2	2	48	3	2				242	3	3
Diaphus brachycephalus	63	9	9	1	1	3		1	3		14	7	1	5	5		3				1	
Diaphus dumerilii	6				2														4			

Table 6 (continued)

Diaphus fragilis	2							2																	
Diaphus lucidus	9	1						4	1		1			1	1										
Diaphus mollis	95	1		1	21		1	17	2	2	3		1	6		2			31	6	1				
Diaphus perspicillatus	5																		1	4					
Diaphus problematicus	39	8	7		2			13		1	4			2	1				1						
Diaphus raffinesquii	3																		3						
Diaphus splendidus	43	12	2		5			4		1	2			13	1	1			2						
Diaphus spec.	1															1									
Hygophum hygomii	11																			11					
Hygophum macrochir	1	1																							
Hygophum reinhardtii	62	7	2					11			8	3		2	4	1				24					
Hygophum taaningi	11	3	1			4	3																		
Hygophum cf. taaningi	20				20																				
H. cf. taaningi/macrochir	205		1		1															203					
Hygophum spec.	2				1			1																	
Lampadena atlantica	104	4	5	5	29	1	2	12	1	2	30	3	1	7	1						1				
Lampanyctus nobilis	25	1	4		8	1		1	1	1	4			3	1										
Lampanyctus photonotus	144		5	2	32	1	1	32	3	1	6			2						54	3	2			
Lampanyctus spec.	5				1					4															
Lepidophanes guentheri	148	1			1			1	1		7	1		5						131					
Lobianchia gemellari	118	15	9	6	5	6	3	5		6	20	3	5	20	4				10		1				
Lobianchia cf. gemellari	16				3			2	11																
Lobianchia spec.	1							1																	
Loweina rara	2										1			1											
Loweina spec.	1										1														
Myctophum nitidulum	8				2			1	1		1	1								2					
Myctophum selenops	21			1	1		1	2			2		6	2	2		1	2	1						
Nannobrachium cuprarium	461	16	27	24			24			32	133	14	5	157	17	7					1	4			
Nannobrachium cf. cuprarium	151				108	27			16																
Nannobrachium lineatum	7				1		2					1		1	2										
Nannobrachium/Lampanyctus	78	7						70	1																
Notoscopelus caudispinosus	29			1	13			6						8	1										
Notoscopelus resplendens	5										1									4					
Symbolophorus rufinus	3							1		1				1											
Taaningichthys minimus	50			4		2			2	3	9	13	8		3	5					1				
Taaningichthys minimus	50			4		2			2	3	9	13	8		3	5					1				
Myctophidae spec.	26	1	2			2		1			3							3	11	2		1			
Osmeriformes																									
Bathylagidae																									
Dolicholagus longirostris	1													1											
Perciformes																									
Bramidae																									
Pteraclis carolinus	9	5						4																	

Table 6 (continued)

Chiasmodontidae																							
Pseudoscopelus altipinnis	6										1				2	2					1		
Pseudoscopelus cf. altipinnis	5									2		3											
Pseudoscopelus spec.	17		1	1	1		3	1	6		1		1								2		
Howellidae																							
Howella brodiei	33	13						7			2			7				2	2				
Nomeidae																							
Cubiceps gracilis	1	1																					
Scombrolabracidae																							
Scombrolabrax heterolepis	62	3	4	1	10	7		9	18	1	5	2		2									
Scombrolabrax cf. heterolepis	7						1	6															
Trichiuridae																							
Trichiuridae spec.	7	3	1							1	2												
Stephanoberyciformes																							
Melamphaidae																							
Melamphaes cf. typhlops	139	1	22	9		5		5	10	16	4	20	11	2	3	16					15		
Melamphaes pumilus	9			2							4				3								
Melamphaes spec.	64	2	5	1	4	1	8	3	1	1	10	15		9	1					2	1		
Poromitra crassiceps	1																					1	
Scopelogadus mizolepis	962		19	42	17	32	72	117	170	74	132	95	7	90	86	9							
Scopelogadus spec.	3																				3		
Melamphaidae spec.	14		2		7	4													1				
Stomiiformes																							
Gonostomatidae																							
Bonapartia pedaliota	67																		57		10		
Cyclothone spec.	9																					9	
Sigmops elongatus	149	7	10	9	1	5	12	4	7	9	11	28	18	9	13	5					1		
Phosichthyidae																							
Ichthyococcus ovatus	1																	1					
Pollichthys mauli	13	2									2							5		4			
Vinciguerria attenuata	7			2			4				1												
Vinciguerria poweriae	4																	4					
Vinciguerria spec.	6	2											1	1	1	1							
Yarella spec.	1				1																		
Phosichthyidae spec.	2	1									1												
Sternoptychidae																							
Argyropelecus aculeatus	64		8	21			10			4		4	11		1	1		1	2		1		
Argyropelecus hemigymnus	2																				2		
Maurolicus weitzmani	2					2																	
Sternoptyx pseudobscura	13																1	2	1			9	
Stomiidae																							
Astronesthes spec.	5							1		1			2	1									
Borostomias cf. mononema	1			1																			
Chauliodus danae	43	2			5			6	2		7	5	1	3							2	10	
Chauliodus cf. danae	6																		6				
Chauliodus sloani	18	2	3	1	1		2		1			3		1							1	3	
Chauliodus spec.	2									2													

Table 6 (continued)

Echiostoma barbatum	6				1						3			1	1				
Echiostoma spec.	1										1								
Eustomias spec.	1	1																	
Leptostomias haplocaulus	1					1													
Leptostomias spec.	6						2	1	1		1				1				
Melanostomias tentaculatus	1											1							
Melanostomias spec.	3						1	2											
Neonesthes capensis	1														1				
Photonectes spec.	2											1	1						
Photostomias guernei	1					1													
Stomias brevibarbatus	4					1				1	1					1			
Idiacanthus fasciola	1									1									
Stomias spec.	1							1											
Stomiidae spec.	2	1														1			
Tetraodontiformes																			
Molidae																			
Masturus lanceolatus	9				2			2	1					1		1			2
Tetraodontidae																			
Canthigaster spec.	14				6			7									1		

quality to any species in identification keys and NCBI Nucleotide Sequence Database). In 19 cases, a genetic confirmation was not possible because the identified taxa were not included in the Database, and in 40 cases, genetic analyses were not performed.

The relative abundance of Myctophidae was high (42.9–67.7% of total catch) in catches from all *regular stations* (stations 228, 240, 259, 284, 300), whereas Melamphaidae showed lower abundances at western stations (stations 228 and 240; 17.4–19.1%) compared to the central and eastern sampling area (stations 259, 284, 300; 31.0–36.7%) (Fig. 7). The dominance of single species in catches was more pronounced in the eastern part of the survey area compared to the west. At the easternmost station (300), the two most abundant species accounted for 51.8% of total catch, while at intermediate stations three species and at the westernmost station (228) six species summed up to 50% of total catch. The share of the two most abundant species increased in catches from west to east (228: 29.1%; 240: 36.8%; 259: 45.4%; 284: 46.0%; 300: 51.8%). Catches at eastern *regular stations* (st. 284 and 300) were dominated by *S. mizolepis* (A=26.2–27.9%), followed by *N. cuprarium* (18.1–25.6%). While *S. mizolepis* also dominated the catch at station 259 (33.3%), *B. photothorax* (17.9%) and *C. warmingii* (19.6%) were the most abundant species in catches from the western stations 228 and 240, respectively. No significant correlations of sea surface temperature and abundance of the four most important species were detected (*S. mizolepis*: t=0.390, p=0.72, R^2=0.05; *N. (cf.) cuprarium*: t=0.31, p=0.77, R^2=0.03; *C. warmingii*: t=2.95, p=0.06, R^2=0.74; *B. photothorax*: t= 0.36, p=0.74, R^2=0.04).

Among *regular stations*, species richness was highest in catches at the northernmost station (station 284), where 50 different species have been caught. *Evermannella indica*, *Macroparalepis brevis*, *Melanostomias tentaculatus*, *Nemichthys scolopaceus* and *Odontostomops normalops* were exclusively caught at that station. Catches at *regular stations* further south contained 44 to 46 different species.

Discussion

The catch composition of mesopelagic fish species during this survey is similar to catches reported from previous investigations in the Sargasso Sea and other North-Atlantic areas (Backus et al. 1969; Ross et al. 2010; Olivar et al. 2017). Stratified night-time catches in layers 1 (epipelagic layer) and 2 (principal DSL) at *regular stations* generally reflected the taxonomic and quantitative composition that was encountered in previous surveys in the eastern part of the Atlantic in the same ecoregion “Central North Atlantic” (Ariza et al. 2016;

Table 7 Length and weight per species and results of genetic analyses. DB database

Species	Standard length (cm)			Weight (g)			Genetic analysis
	N	Mean	SD	N	Mean	SD	
Anoplogaster spec.	34	2.3	0.6	34	1	0.6	Confirmed
Argyropelecus aculeatus	61	5	1.0	63	4.9	3.1	Confirmed
Argyropelecus hemigymnus	1	2.2	0.0	1	0.2		Not tested
Astronesthes spec.	5	10.6		5	9.8	8.0	Confirmed
Bolinichthys indicus	22	3.4	0.3	20	0.5	0.2	Confirmed
Bolinichthys photothorax	307	5.5	0.8	303	2.2	0.8	Confirmed
Bolinichthys spec.	3	4.6	3.4	3	2.5	3.9	Confirmed
Bonapartia pedaliota	66	5.6	0.5	66	1.3	0.3	Confirmed
Borostomias cf. mononema	1	8.3		1	3.1		Not tested
Bregmaceros spec.	26	6.9	1.3	26	2.5	1.4	Not in DB
Canthigaster spec.	14	0.9	0.2	9	0.1	0.1	Not in DB
Ceratoscopelus warmingii	633	5.5	1.0	633	2.2	1.0	Confirmed
Chauliodus cf. danae	5	6.7	1.8	5	0.8	0.2	Not tested
Chauliodus danae	37	10.3	2.2	39	2.1	1.7	Confirmed
Chauliodus sloani	16	17.2	5.6	15	28	49.0	Confirmed
Chauliodus spec.	1	10.7		1	2.3		Not tested
Coccorella atlantica	62	7.3	2.3	62	4.4	6.2	Confirmed
Cubiceps gracilis	0			0			Not tested
Cyclothone spec.	9	4.6	0.5	9	0.3	0.1	Confirmed
Derichthys serpentinus	1	7		1	0.1		Confirmed
Diaphus brachycephalus	60	3.9	0.4	59	1.2	0.3	Confirmed
Diaphus dumerilii	6	5.3	0.4	6	1.7	0.5	Not in DB
Diaphus effulgens	6	4.2	1.3	6	1.8	3.1	Confirmed
Diaphus fragilis	2			2			Confirmed
Diaphus lucidus	9	6	1.1	8	3.6	1.9	Confirmed
Diaphus mollis	95	4	0.5	94	0.9	0.3	Confirmed
Diaphus perspicillatus	5	5.5	0.8	5	3.2	1.1	Confirmed
Diaphus problematicus	39	6.7	0.8	31	4.9	1.3	Not in DB
Diaphus raffinesquii	3	8.4	0.4	3	9	0.8	Confirmed
Diaphus spec.	1	4.8		1	2.1		Not tested
Diaphus splendidus	43	6	0.7	31	2.8	1.0	Confirmed
Diretmoides spec.	3	5.2	1.4	3	6.6	3.9	Confirmed
Dolicholagus longirostris	1	8		1	1.5		Confirmed
Echiostoma barbatum	6	17.5	2.1	6	19	6.0	Confirmed
Echiostoma spec.	0			0			Not tested
Eustomias spec.	0			0			Confirmed
Evermannella indica	1	7.1		1	2.3		Not tested
Evermannellidae spec.	2			2			Not tested
Howella brodiei	11	5	0.9	11	2.8	2.0	Confirmed
Hygophum cf. taaningi	18	3.5	0.5	19	0.5	0.3	Not tested
H. cf. taaningi/macrochir	192	3.3	0.5	199	0.5	0.3	Not tested
Hygophum hygomii	11	4.7	0.3	11	1.6	0.5	Not tested
Hygophum macrochir	1	3.6		0			Not tested
Hygophum reinhardtii	58	3.4	0.4	49	0.4	0.2	Confirmed
Hygophum spec.	1	4.3	1.1	1	1		Confirmed
Hygophum taaningi	11	3.5	0.5	8	0.8	0.3	Confirmed
Ichthyococcus ovatus	1	1.7		0			Not tested
Idiacanthus fasciola	1	23		1	1.4		Confirmed
Lampadena atlantica	103	5.8	1.6	102	3.1	2.7	Confirmed
Lampanyctus nobilis	25	9.8	1.1	24	8	2.8	Confirmed
Lampanyctus photonotus	142	5.5	0.5	143	1.5	0.5	Confirmed
Lampanyctus spec.	4	5.9	3.5	5	2.1	2.4	Not tested
Lepidophanes guentheri	142	3.6	1.1	93	0.5	0.7	Confirmed
Leptostomias haplocaulus	1	16.3		1	6.9		Not tested
Leptostomias spec.	4	18.8	5.9	4	11.4	7.0	Not in DB
Lestidiops spec.	15	9.4	1.8	15	2	1.1	Not in DB
Lobianchia cf. gemellari	16	4.5	0.6	16	1.4	0.5	Not tested
Lobianchia gemellari	113	4.7	0.6	102	1.6	0.6	Confirmed
Lobianchia spec.	1	4.3		1	0.9		Not tested
Loweina rara	2			2			Not tested
Loweina spec.	1	3.5		1	0.4		Not in DB
Macroparalepis brevis	1	11		1	2.4		Not tested
Masturus lanceolatus	8	0.7	0.3	5	0.1	0.0	Confirmed

Table 7 (continued)

Species	Standard length (cm)			Weight (g)			Genetic analysis
	N	Mean	SD	N	Mean	SD	
Maurolicus weitzmani	2			2			Not tested
Melamphaes cf. typhlops	124	4.1	0.6	134	1.5	0.7	Not in DB
Melamphaes pumilus	5	2	0.1	3	0.1	0.0	Not tested
Melamphaes spec.	61	2.2	0.8	59	0.3	0.6	Not in DB
Melamphaidae spec.	6	1.8	0.2	0			Not in DB
Melanocetus johnsonii	1	8.6		1	62		Confirmed
Melanonus zugmayeri	3	10.7	2.0	3	7.3	3.8	Confirmed
Melanostomias spec.	3	10.4	3.4	3	3.6	4.2	Not in DB
Melanostomias tentaculatus	1	16.1		1	8.1		Not in DB
Myctophidae spec.	21	4.1	1.7	21	1.4	2.1	Not tested
Myctophum nitidulum	8	6.1	0.9	8	3.6	1.6	Confirmed
Myctophum selenops	21	6	1.1	21	4.8	2.0	Confirmed
Nannobrachium cf. cuprarium	146	6.2	0.9	146	1.3	0.5	Not tested
Nannobrachium cuprarium	448	6.4	0.8	444	1.5	0.5	Confirmed
Nannobrachium lineatum	4	10.3	1.6	4	4.4	1.8	Confirmed
Nannobrachium/Lampanyctus	74	6.2	1.2	74	1.3	0.7	Not tested
Nemichthys scolopaceus	0			1	16.2		Not tested
Neonesthes capensis	1	10.6		1	6.8		Confirmed
Notoscopelus caudispinosus	29	8.6	0.5	29	8.8	1.8	Confirmed
Notoscopelus resplendens	5	8.1	1.1	5	7.2	2.9	Confirmed
Odontostomops normalops	1	8.2		1	4.8		Confirmed
Paralepididae spec.	0			0			Not tested
Phosichthyidae spec.	1	3		1	0.2		Not tested
Photonectes spec.	2			2			Not in DB
Photostomias guernei	1	7.4		1	1.2		Confirmed
Pollichthys mauli	12	4	0.4	12	0.2	0.1	Confirmed
Poromitra crassiceps	1	10.5		1	17.5		Confirmed
Pseudoscopelus altipinnis	5	8.6	0.6	5	5.9	2.2	Not in DB
Pseudoscopelus cf. altipinnis	5	8	1.1	5	5.6	2.4	Not in DB
Pseudoscopelus spec.	16	7.7	2.0	16	5	3.8	Not tested
Pteraclis carolinus	4	4.6	1.3	4	2	1.6	Not in DB
Scombrolabrax cf. heterolepis	7	4.7	0.7	7	1.5	0.5	Not tested
Scombrolabrax heterolepis	55	5.2	2.2	55	3.3	9.9	Confirmed
Scopelarchus analis	2			2			Not tested
Scopelarchus spec.	9	5.1	1.3	9	2	1.4	Confirmed
Scopelogadus mizolepis	884	4.9	0.9	924	1.8	1.1	Confirmed
Scopelogadus spec.	0			2			Not tested
Scopelosaurus smithii	26	9.6	2.6	26	4	3.2	Not in DB
Scopelosaurus spec.	1	10.3		1	4		Not tested
Serrivomer beanii	0			4	10.8	8.4	Confirmed
Serrivomeridae spec.	1	15.3		1	0.6		Not tested
Sigmops elongatus	144	13.2	3.0	144	8	6.5	Confirmed
Sternoptyx pseudobscura	13	2.4	0.3	13	0.6	0.2	Confirmed
Stomias brevibarbatus	4	14.2	2.2	4	7.6	3.3	Not in DB
Stomias spec.	1	9.4		1	1.7		Not tested
Stomiidae spec.	1	9.7		1	4.3		Not tested
Sudis spec.	3	8	1.8	3	2.4	1.8	Confirmed
Symbolophorus rufinus	3	7.9	0.5	3	7.6	1.7	Confirmed
Taaningichthys minimus	50	4.1	0.7	50	0.8	1.2	Confirmed
Trichiuridae spec.	3	22.6	10.7	3	16.9	24.6	Not in DB
Vinciguerria attenuata	3	2.8	0.5	2			Not tested
Vinciguerria poweriae	3	2.6	0.1	4	0.1	0.1	Not tested
Vinciguerria spec.	4	3.6	0.3	4	0.3	0.1	Not tested
Yarella spec.	1	5.7		1	0.6		Not tested

Olivar et al. 2017; Sutton et al. 2017). It is known that organisms from epi- and upper mesopelagic layers exhibit strong DVM and generally show the strongest differences in day- and night-time distribution with aggregations in the epipelagic zone during night (Roe and Badcock 1984; Olivar et al. 2017). This diel vertical migrating functional group also comprises — among others — Gonostomatidae, Sternoptychidae, Phosichthyidae and Stomiidae, together with invertebrate micronekton (crustaceans and molluscs) (Sutton 2013). In this study, different components of the migrating group constituting the bulk of catches originate from different zones of the mesopelagial: while many of the sampled myctophids can be considered to originate from the principal DSL (layer 2), other taxonomic groups like melamphaids and some gonostomatids and sternoptychids are expected to have migrated from the deeper secondary DSL (layer 3). As found in previous studies, species of the family Melamphaidae are characteristic of the deeper mesopelagic fish community and usually show maximum concentrations between 400 and 800 m during the day and a more widespread distribution during night-time (Barlow and Sutton 2008; Sutton et al. 2008; Sutton 2013; Olivar et al. 2017). Some gonostomatid species are not known to display extensive DVM and usually are found in layers below the epipelagial both during day- and night-time (McClain et al. 2001; Olivar et al. 2017). While in this study similar observations were also made from the deep hauls, where Gonostomatidae were sampled in the corresponding layers, the species sampled in epipelagic night-time catches are characteristic of the upper mesopelagic zone and are known to undertake DVM (Sutton 2013). The here presented catches of stomiids reflected their known distribution and migration pattern as previously reported by Kenaley (2008) and Olivar et al. (2017), with night catches of individual specimens in layer 1, while during day-time this family was only sampled below 400 m depth. The comparatively large number of species of the subfamily Melanostomiinae caught in this study during night-time in layers 1 and 2 is a further indication of vertical migration behaviour in these

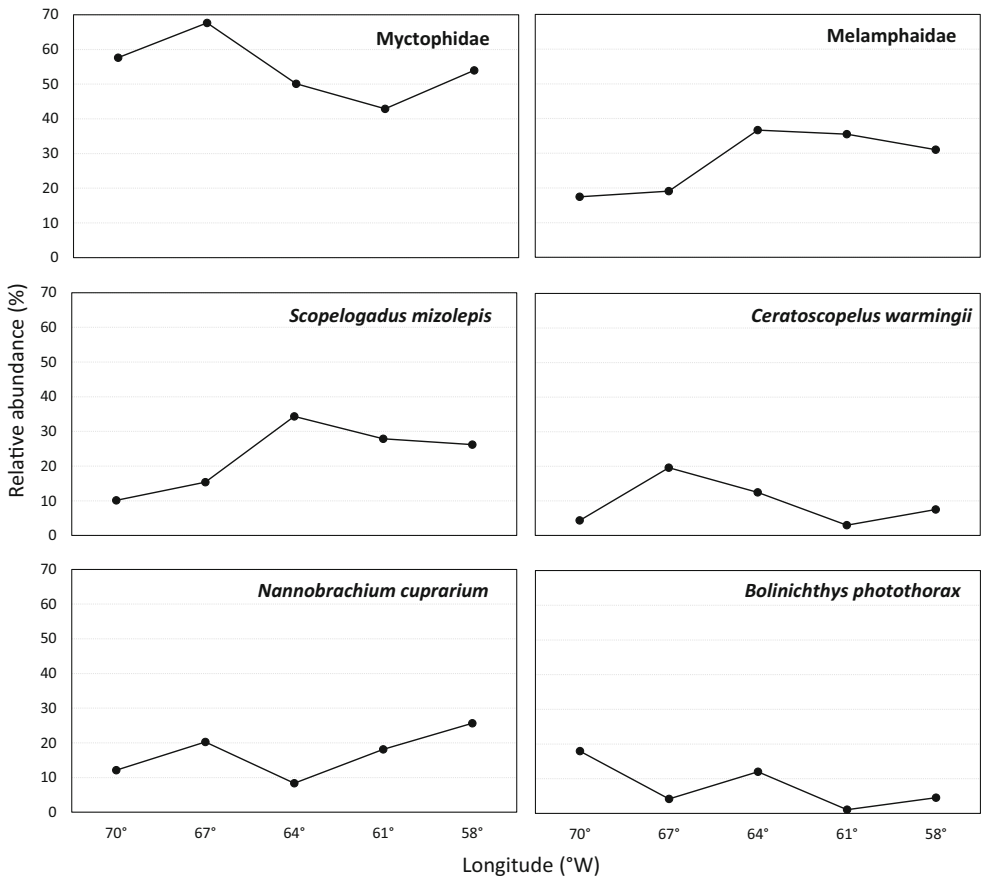

Fig. 7 Relative abundance of Myctophidae and Melamphaidae and the four most abundant species (*Scopelogadus mizolepis, Ceratoscopelus warmingii*, *Nannobrachium cuprarium*, *Bolinichthys photothorax*) in catches at geographical longitude

species. This corroborates accumulating evidence from oligotrophic, but also productive regions, that these species, despite remaining likely invisible in hydroacoustic recordings, contribute considerably to vertical energy fluxes (Cook et al. 2013; Eduardo et al. 2020a; Czudaj et al. submitted). Sternoptychidae in general are considered limited or only partial migrants (Kinzer and Schulz 1988) and usually occur preferentially in deeper layers, although some shallower occurrences can be observed during night hauls, especially in oligotrophic regions as shown for the south western Atlantic (Olivar et al. 2017; Eduardo et al. 2020b). This is well in line with the observations in this study, as night-time catches of sternoptychids, mainly dominated by *Argyopelecus aculeatus*, were present in the deeper nets of the epipelagic zone (below layer 1) and also occurred in layers 2 and 3 both during day and night (Table 6). The general observation of characteristic scattering layers in different depths in this study that show rather unique backscattering characteristics and regular DVM of organisms originating from different depth zones, was consistent with observations from adjacent areas and also from across the pelagic zones of the global ocean (Sutton 2013; Peña et al. 2014; Ariza et al. 2016; D'Elia et al. 2016; Klevjer et al. 2016). The observed presence of an epipelagic layer (layer1), a strong upper mesopelagic deep scattering layer (layer 2, principal DSL) as well as a weaker lower deep scattering layer (layer 3, secondary DSL) was in line with general descriptions of the ocean's deep mesopelagic zone (Proud et al. 2017). The detected layers with different scattering properties highly resembled layers characterized at the Canary Islands in the eastern Atlantic and the Northeastern Atlantic in general: an epipelagic layer with strong diel differences in scattering characteristics; a stationary upper layer of the upper principal DSL (upper layer 2) dominated by 18 kHz (450–550 m); a stationary lower layer of the principal DSL (layer 2) with a dominance of 38 kHz (ca. 600–700 m) and a mixed layer between; weak or no signals between 700 and 800 m; a permanent weak layer dominant at 18 kHz (secondary DSL, layer 3) between ca. 800 and 1000 m (Ariza et al. 2016; Klevjer et al. 2016). Additionally, similar patterns of a different but recurrent temporal onset of DVM of groups with differing backscattering characteristics at nightfall and the later descent into deeper layers with sunrise, as shown in this study, have been observed in nearby regions to the southwest (D'Elia et al. 2016) and east (Ariza et al. 2016) of the survey area. However, in this study, the sampling regime did not allow targeting and resolving the different upward and downward migrating fractions from different layers or the composition of the different layers itself. Nonetheless, based on the backscattering characteristics, and in comparison with previous studies, it seems likely that the upper part of the principal DSL (layer 2) mostly consisted of small, swimbladdered fishes resonant at 18 kHz like myctophids that also contributed the bulk of migrating fish emerging from that layer at nightfall (Peña et al. 2014, 2020; Ariza et al. 2016). While the lower part of the principal DSL (layer 2) remained rather stationary, migrant fauna also contributed to this layer, albeit to a lower extent. Although it was only caught in low numbers in this study, the gonostomatid *Cyclothone* spp. seem to be the dominant fish in the principal DSL (layer 2) (compare Ariza et al. (2016)). In contrast to Ariza et al. (2016) and Sutton (2013), who described the lower mesopelagic zone/secondary DSL (800–1000 m) as permanent and stationary, but identified a weak migrant signal between 700 and 800 m that disappeared at night, in this study a migrant pathway clearly became visible emerging from the secondary DSL (layer 3) and migrating upward through the principal DSL (layer 2), with no clear changes in the signal of the stationary fraction of that zone. Based on the dominance of the 18 kHz echoes, it can be assumed that the migrating and the stationary signal also originate from swimbladdered fishes and gas-bearing organisms. From that layer not only a peak in non-migrant fishes like *Cyclothone* spp. was reported earlier, but also of migrating fishes like the myctophid *Notoscopelus* spp. (Badcock and Merrett 1976; Roe and Badcock 1984; Sutton 2013; Ariza et al. 2016). The latter have — among others — contributed to epipelagic night-time catches made during this study. It has to be mentioned that a certain amount of backscattering in the lower frequency range also is highly likely to originate from physonect siphonophores carrying a gas-filled pneumatophore for buoyancy (Kloser et al. 2016; Proud et al. 2019). While comparatively little is known on actual vertical distribution or migration of these organisms (Pugh 1975; Pugh 1984; Lüskow et al. 2019), siphonophores are known to inhabit a broad depth range in the epi- as well as the upper mesopelagial, and some species also undertake DVM. Despite gelatinous zooplankton not being identified to lower taxonomic levels due to the fragility of the organisms and their condition in the codend of the multisampler nets, the contribution of gelatinous zooplankton to the total catch weight especially in the deep tows (net 3 of stations 233

(450–698 m) and 316 (774–965 m)) indicates that a certain fraction of the scattering layers with a dominance at 18 and 38 kHz may be assigned to a contribution from siphonophores.

The presence and condition of swimbladders changes among and within taxonomic groups of mesopelagic fish — and even may vary within genera and species based on developmental stage and length (Marshall 1960). It has been shown that e.g. biomass estimates of mesopelagic fish based on acoustic data collected at 38 kHz can be complicated because of the small physical size of mesopelagic fauna, ontogenetic changes in swimbladder morphology, inflation and regression (Davison et al. 2015). Additionally, the backscatter is depth-sensitive and non-linear with respect to size; at the same time, the size structure of mesopelagic fish is skewed with abundance driven by the smallest and biomass driven by the largest fishes. Echograms accordingly rather reflect the distribution of the strongest scatterers — e.g. (small) fishes with swimbladders — than the actual distribution of biomass (Davison et al. 2015). While some of the individual species identified in the multinet hauls may have different swimbladder characteristics than other genera/species from the same family, it is assumed that the main drivers of backscatter characteristics of scattering layers are still correctly identified through the classification used in this study.

A classification of hydroacoustic data into categories based on their scattering properties (e.g. D´Elia et al. 2016) and in combination with trawl net hauls is feasible, but a comprehensive interpretation of the aggregated results is challenging and corresponding sampling biases have been reported (Kaartvedt et al. 2012). This also affects contributions of gelatinous zooplankton and other invertebrates that may significantly contribute to backscatter through resonance at low frequencies but will be virtually absent from trawl haul catches due to the small and/or fragile nature of these organisms. It can safely be assumed that the corresponding layers identified using the method described by D'Elia et al. (2016) are not exclusively inhabited by the dominant taxonomic groups triggering the classification, but also by a magnitude of other species whose acoustic signal is masked by the dominant scatterers as well as the range limitation inherent in hydroacoustic data from higher frequencies. An indication for such a masking and/or a "missed classification" is evident from the catch composition of some tows that were conducted within layers with typical characteristics and dominance of gas-bearing organisms (i.e. resonant at 18 and 38 kHz), but also contained fluid-like zooplankton organisms like crustaceans and molluscs. As the scientific echosounder could not be calibrated directly prior to, during or after the survey, but had been calibrated with good results on a previous survey and was again calibrated a few weeks after the survey, the utilization of transducer parameters from a preceding calibration updated with ambient physical measurements from the current survey is considered sufficiently precise for the classification attempted here. The classification approach followed in this study is based on Sv intervals that are used to differentiate biological groups. D'Elia et al. (2016) derived the corresponding parameters from length measurements of representative organisms from concurrent net samples and on theoretical models relating these lengths to target strengths and subsequently to the Δ_{Sv} intervals. Since this study was conducted in a different, albeit adjacent, ecoregion with potentially different species and length compositions (e.g. Sutton et al. 2017), a certain degree of misclassification cannot be ruled out. Cells that did not match Δ_{Sv} intervals specified in D'Elia et al. (2016) could nevertheless be allocated to e.g. swimbladder-bearing fishes based on their scattering properties (Love 1978). Accordingly, the overall classification is considered robust enough for the analyses conducted.

According to Backus et al. (1970), who defined oceanic areas in the Atlantic on the basis of characteristic water masses, and supported by the hydrographic data obtained during this survey, the here investigated area is part of the Southern Sargasso Sea. This zone is characterized by distinct temperature fronts (Fig. 1), which are present from fall to spring (Halliwell et al. 1991). In this study, species richness was slightly higher at the northernmost station (lowest SST) compared to warmer stations further south with five species exclusively caught at the northernmost station. However, since only single individuals of these species were caught, the observed higher species richness north of the front might also be an artefact of low sampling effort. Nonetheless, similar results were reported by Backus et al. (1969), who caught a number of species north of the temperature front that were absent further south. In this study, northern and southern fish communities could not be compared in detail, since the sampling grid was not designed accordingly, but the total survey area comprised the Central Atlantic Mesopelagic Ecoregion that in general has a distinct faunal composition, albeit with spatial differences that are based primarily on abundance and rank order rather than presence or absence of species (Sutton et al. 2017).

Variations were observed between eastern and western stations with regard to the predominant species in catches (i.e.

S. mizolepis and *N. cuprarium* vs. *B. photothorax* and *C. warmingii*). These differences were apparently not driven by water temperature, since no significant correlation was evident between SST and the abundance of the four most abundant fish species. However, in case of *C. warmingii* (p=0.06, R^2=0.74), the absence of a significant correlation might be the result of the limited number of sampling stations. The relevance of temperature as a major driver for fish distribution might be lower in species that experience strong temperature gradients on a daily basis caused by DVM. Other environmental conditions like primary production, oxygen concentration and light attenuation where also shown to affect the distribution of mesopelagic fish species (Irigoien et al. 2014; Klevjer et al. 2016; Aksnes et al. 2017), but were not analysed in this study. Hence, the SST data collected in this study do not provide a full picture of environmental influences on the mesopelagic fish community, but contain information about the potential effect of horizontal temperature structures like temperature fronts on the distribution of mesopelagic fish. Nonetheless, the absence of a temperature effect on changes in the distribution of the dominant species suggests that the here observed changes in catch composition reflect differing regional influences from adjacent water masses.

Due to methodological constraints in sampling (large mesh size, relatively small number of stations, sampling not only in peak scattering layers), the data obtained and presented here do not provide a fully comprehensive and representative picture of the mesopelagic species composition of the investigated area. Stations, catch depths and trawl paths of this study were defined by the needs of the original purpose of the survey and not for the investigation of the mesopelagic fish community, which was only an additional benefit of the survey. As a consequence, no day-time samples were collected from the epipelagic scattering layer (layer 1) and the deep scattering layers (layers 2 and 3) could only be sampled at two stations at the far ends of the survey area. This study design hampers the discernibility of permanent residents and migrators in the different layers and complicates a more detailed interpretation of catches with regard to DVM. Another limitation of this study is the relatively large mesh size of the mesopelagic trawl. This might have led to the under-representation of certain small and thin species in catches, despite a general capture efficiency of the gear also for small-sized species < 30 mm (Fock and Czudaj 2018). For example, bristlemouths of the genus *Cyclothone* are usually found in high abundance in the investigated area and have been reported as resonant scatterers at depth (Peña et al. 2014). In this study, *Cyclothone* represents only a minor fraction of the trawl samples, which most likely is due to the large mesh sizes in the codend of the trawl net employed (1.5 cm), as it already was the case in the eastern tropical North Atlantic (Fock and Czudaj 2018; Czudaj et al. submitted). Large mesh sizes may also be the reason why *Ranzania laevis*, a small species of the sunfish family Molidae, was not present in any of the hauls, even though spawning activity and increased larval and post-larval abundance during the March and April in the area were recently described by Hellenbrecht et al. (2019). It is noteworthy though that nine post-larval (Molacanthus stage) specimens of *Masturus lanceolatus*, another fairly unexplored species of Molidae, were caught in this study.

Despite aforementioned limitations, the current study provides valuable insights into the distribution and vertical migration behaviour of mesopelagic fishes in the Sargasso Sea and adds to our understanding of the mesopelagic community in this large oceanic area. To assess how and to what extent the fish community in this ecoregion is affected by the influence of adjacent areas and by (changing) hydrographic conditions requires additional effort and extensive further investigations.

Acknowledgements Captain and crew of the R/V Walther Herwig III are acknowledged for their helpful cooperation during the survey. Thanks also go to Katrin Unger, Katsumi Tsukamoto, Michael J. Miller, Shun Watanabe, Håkan Westerberg and Holger Ossenbrügger for their help during sampling. Two anonymous reviewers are acknowledged for their thorough revision of the manuscript and their very valuable comments, corrections and recommendations.

Funding Open Access funding enabled and organized by Projekt DEAL. The R/V Walther Herwig III survey was funded by the German Federal Ministry of Food and Agriculture.

Declarations

Conflict of interest The authors declare no competing interests.

Ethical approval All necessary permits for sampling and observational field studies have been obtained by the authors from the competent authorities and are mentioned in the acknowledgements, if applicable.

Sampling and field studies All necessary permits for sampling and observational field studies have been obtained by the authors from the competent authorities and are mentioned in the acknowledgements, if applicable. The study is compliant with CBD and Nagoya protocols.

Data availability The datasets generated during and/or analysed during the current study are available from the corresponding author on request

Author contributions LM and MS conceived and designed research and analysed the data. LM, MF, JP, KW, SC and RH conducted morphological species identification. MF and JP analysed CTD and SST data. TB made genetic analyses. All authors contributed to manuscript writing and read and approved the manuscript.

References

Aksnes DL, Røstad A, Kaartvedt S, Martinez U, Duarte CM, Irigoien X (2017) Light penetration structures the deep acoustic scattering layers in the global ocean. Sci Adv 3:e1602468

Altschul SF, Gish W, Miller W, Myers EW, Lipman DJ (1990) Basic local alignment search tool. J Mol Biol 215:403–410

Anderson TR, Martin AP, Lampitt RS, Trueman CN, Henson SA, Mayor DJ (2019) Quantifying carbon fluxes from primary production to mesopelagic fish using a simple food web model. ICES J Mar Sci 76:690–701

Ariza A, Landeir JM, Escánez A, Wienerroither R, Aguilar de Soto N, Røstad A, Kaartvedt S et al (2016) Vertical distribution, composition and migratory patterns of acoustic scattering layers in the Canary Islands. J Mar Syst 157:82–91

Ayala A, Riemann L, Munk P (2016) Species composition and diversity of fish larvae in the subtropical convergence zone of the Sargasso Sea from morphology and DNA barcoding. Fish Oceanogr 23:85–104

Backus R, Craddock J (1977) Pelagic faunal provinces and sound-scattering levels in the Atlantic Ocean. Oceanic sound scattering prediction 529-547.

Backus RH, Craddock J, Haedrich R, Shores D (1969) Mesopelagic fishes and thermal fronts in the western Sargasso Sea. Mar Biol 3: 87–106

Backus RH, Craddock JE, Haedrich RL, Shores DL (1970) The distribution of mesopelagic fishes in the equatorial and western North Atlantic ocean. J Mar Res 28:179–201

Badcock J, Merrett NR (1976) Midwater fishes in the eastern North Atlantic—I. Vertical distribution and associated biology in 30°N, 23°W, with developmental notes on certain myctophids. Prog Oceanogr 7:3–58

Barlow K, Sutton T (2008) Ecology of the midwater fish family Melamphaidae over the Mid-Atlantic Ridge. ICES CM 100:17

Bianchi D, Mislan KAS (2016) Global patterns of diel vertical migration times and velocities from acoustic data. Limnol Oceanogr 61:353–364

Carpenter KE (2002) The living marine resources of the Western Central Atlantic. Three Volume Set., FAO Rome.

Cook AB, Sutton TT, Galbraith JK, Vecchione M (2013) Deep-pelagic (0–3000m) fish assemblage structure over the Mid-Atlantic Ridge in the area of the Charlie-Gibbs Fracture Zone. Deep-Sea Res II 98: 279–291

Craddock JE, Backus RH, Daher MA (1992) Vertical distribution and species composition of midwater fishes in warm-core Gulf Stream meander/ring 82-H. Deep Sea Res I 39:203–218

Czudaj S, Koppelmann R, Schaber M, Möllmann C, Fock H (submitted) Community structure of mesopelagic fishes constituting sound scattering layers in the eastern tropical North Atlantic – vertical functional differences related to productivity and oxygen minimum conditions

Davison PC, Checkley DM Jr, Koslow JA, Barlow J (2013) Carbon export mediated by mesopelagic fishes in the northeast Pacific Ocean. Prog Oceanogr 116:14–30

Davison PC, Koslow JA, Kloser RJ (2015) Acoustic biomass estimation of mesopelagic fish: backscattering from individuals, populations, and communities. ICES J Mar Sci 72:1413–1424

De Robertis A, Higginbotto I (2007) A post-processing technique to estimate the signal-to-noise ratio and remove echosounder background noise. ICES J Mar Sci 64:1282–1291

D'Elia M, Warren JD, Rodriguez-Pinto I, Sutton TT, Cook A, Boswell KM (2016) Diel variation in the vertical distribution of deep-water scattering layers in the Gulf of Mexico. Deep Sea Res I 115:91–102

Demer DA, Berger L, Bernasconi M, Bethke E, Boswell KM, Chu DZ, Domokos R et al (2015) Calibration of acoustic instruments. ICES Coop Res Rep 326:1–136

Eden BR, Steinberg DK, Goldthwait SA, McGillicuddy DJ (2009) Zooplankton community structure in a cyclonic and mode-water eddy in the Sargasso Sea. Deep Sea Res I 56:1757–1776

Eduardo LN, Lucena-Frédou F, Mincarone MM, Soares A, Le Loc'h F, Frédou T, Ménard F et al (2020a) Trophic ecology, habitat, and migratory behaviour of the viperfish Chauliodus sloani reveal a key mesopelagic player. Sci Rep 10:20996

Eduardo LN, Bertrand A, Mincarone MM, Santos LV, Frédou T, Assunção RV, Silva A et al (2020b) Hatchetfishes (Stomiiformes: Sternoptychidae) biodiversity, trophic ecology, vertical niche partitioning and functional roles in the western Tropical Atlantic. Prog Oceanogr 187:102389

Fock HO, Czudaj S (2018) Size structure changes of mesopelagic fishes and community biomass size spectra along a transect from the equator to the Bay of Biscay collected in 1966–1979 and 2014–2015. ICES J Mar Sci 76:755–770

Foote KG, Knudsen HP, Vestnes G, MacLennan DN, Simmonds EJ (1987) Calibration of acoustic instruments for fish density estimation: a practical guide. ICES Coop Res Rep 144:1–81

FWNA (1989) Fishes of the Western North Atlantic 1948-1989. Nine Volume Set, Sears Foundation for Marine Research, Yale University.

Gartner JV Jr, Steele P, Torres J (1989) Aspects of the distribution of lanternfishes (Pisces: Myctophidae) from the Northern Sargasso Sea. B Mar Sci 45:555–563

Godø OR, Samuelsen A, Macaulay GJ, Patel R, Hjøllo SS, Horne J, Kaartvedt S et al (2012) Mesoscale eddies are oases for higher trophic marine life. PLoS One 7:e30161

Halliwell GR, Cornillon P, Brink KH, Pollard RT, Evans DL, Regier LA, Toole JM et al (1991) Descriptive oceanography during the Frontal Air-Sea Interaction Experiment: Medium-to large-scale variability. J Geophys Res Oceans 96:8553–8567

Hansell DA, Carlson CA (2001) Biogeochemistry of total organic carbon and nitrogen in the Sargasso Sea: control by convective overturn. Deep-Sea Res II 48:1649–1667

Hellenbrecht L, Freese M, Pohlmann J, Westerberg H, Blancke T, Hanel R (2019) Larval distribution of the ocean sunfishes *Ranzania laevis* and *Masturus lanceolatus* (Tetraodontiformes: Molidae) in the Sargasso Sea subtropical convergence zone. J Plankton Res 41: 595–608

Irigoien X, Klevjer TA, Røstad A, Martinez U, Boyra G, Acuña JL, Bode A et al (2014) Large mesopelagic fishes biomass and trophic efficiency in the open ocean. Nat Commun 5:3271

Ivanova NV, Zemlak TS, Hanner RH, Hebert PDN (2007) Universal primer cocktails for fish DNA barcoding. Mol Ecol Notes 7:544–548

Jahn AE, Backus RH (1976) On the mesopelagic fish faunas of Slope Water, Gulf Stream, and northern Sargasso Sea. In Deep Sea Research and Oceanographic Abstracts 223-234. Elsevier..

Kaartvedt S, Staby A, Aksnes DL (2012) Efficient trawl avoidance by mesopelagic fishes causes large underestimation of their biomass. Mar Ecol Prog Ser 456:1–6

Katz EJ (1969) Further study of a front in the Sargasso Sea. Tellus 21: 259–269

Kenaley CP (2008) Diel vertical migration of the loosejaw dragonfishes (Stomiiformes : Stomiidae : Malacosteinae): a new analysis for rare pelagic taxa. J Fish Biol 73:888–901

Kinzer J, Schulz K (1988) Vertical distribution and feeding patterns of midwater fish in the central equatorial Atlantic II. Sternoptychidae. Mar Biol 99:261–269

Klevjer TA, Irigoien X, Røsta A, Fraile-Nuez E, Benítez-Barrios VM, Kaartvedt S (2016) Large scale patterns in vertical distribution and behaviour of mesopelagic scattering layers. Sci Rep 6:19873

Kloser RJ, Ryan TE, Keith G, Gershwin L (2016) Deep-scattering layer, gas-bladder density, and size estimates using a two-frequency acoustic and optical probe. ICES J Mar Sci 73:2037–2048

Korneliussen RJ, Ona E (2003) Synthetic echograms generated from the relative frequency response. ICES J Mar Sci 60:636–640

Laffoley DdA, Roe H, Angel M, Ardron J, Bates N, Boyd I, Brooke S et al (2011) The protection and management of the Sargasso Sea: the golden floating rainforest of the Atlantic Ocean. Summary Science and Supporting Evidence Case. Sargasso Sea Alliance, 44 pp.

Lam VWY, Pauly D (2005) Mapping the global biomass of mesopelagic fishes. Sea Around Us Project Newslett 30:4

Li C, Orti G, Zhang G, Lu G (2007) A practical approach to phylogenomics: the phylogeny of ray-finned fish (Actinopterygii) as a case study. BMC Evol Biol 7:44

Lischka A, Piatkowski U, Hanel R (2017) Cephalopods of the Sargasso Sea: distribution patterns in relation to oceanography. Mar Biodivers 47:685–697

Love RH (1978) Resonant acoustic scattering by swimbladder-bearing fish. J Acoust Soc Am 64:571–580

Lüskow F, Neitzel P, Miller MJ, Marohn L, Wysujack K, Freese M, Pohlmann JD, Hanel R (2019) Distribution and abundance of net-captured calycophoran siphonophores and other gelatinous zooplankton in the Sargasso Sea European eel spawning area. Mar Biodivers 49:2333–2349

Marshall NB (1960) Swimbladder structure of deep-sea fishes in relation to their systematics and biology. Discov Rep 31:1–122

Maximenko N, Hafner J, Niiler P (2012) Pathways of marine debris derived from trajectories of Lagrangian drifters. Mar Pollut Bull 65:51–62

McClain CR, Fougerolle MF, Rex MA, Welch J (2001) MOCNESS estimates of the size and abundance of a pelagic gonostomatid fish Cyclothone pallida off the Bahamas. J Mar Biol Assoc UK 81:869–871

McGillicuddy D, Robinson A, Siegel D, Jannasch H, Johnson R, Dickey T, McNeil J et al (1998) Influence of mesoscale eddies on new production in the Sargasso Sea. Nature 394:263–266

Netburn AN, Koslow JA (2018) Mesopelagic fish assemblages across oceanic fronts: a comparison of three frontal systems in the southern California Current Ecosystem. Deep Sea Res I 134:80–91

Olivar MP, González-Gordillo JI, Salat J, Chust G, Cózar A, Hernández-León S, Fernández de Puelles ML et al (2016) The contribution of migratory mesopelagic fishes to neuston fish assemblages across the Atlantic, Indian and Pacific Oceans. Mar Freshw Res 67:1114–1127

Olivar MP, Hulley PA, Castellón A, Emelianov M, López C, Tuset VM, Contreras T et al (2017) Mesopelagic fishes across the tropical and equatorial Atlantic: biogeographical and vertical patterns. Prog Oceanogr 151:116–137

Olson DB, Backus RH (1985) The concentrating of organisms at fronts: a cold-water fish and a warm-core Gulf Stream ring. J Mar Res 43: 113–137

Palter JB, Lozier MS, Barber RT (2005) The effect of advection on the nutrient reservoir in the North Atlantic subtropical gyre. Nature 437: 687–692

Peña M, Olivar MP, Balbín R, López-Jurado JL, Iglesias M, Miquel J (2014) Acoustic detection of mesopelagic fishes in scattering layers of the Balearic Sea (western Mediterranean). Can J Fish Aquat Sci 71:1186–1197

Peña M, Cabrera-Gámez J, Domínguez-Brito AC (2020) Multi-frequency and light-avoiding characteristics of deep acoustic layers in the North Atlantic. Mar Environ Res 154:104842

Proud R, Cox MJ, Brierley AS (2017) Biogeography of the Global Ocean's Mesopelagic Zone. Curr Biol 27:113–119

Proud R, Handegard NO, Kloser RJ, Cox MJ, Brierley AS (2019) From siphonophores to deep scattering layers: uncertainty ranges for the estimation of global mesopelagic fish biomass. ICES J Mar Sci 76: 718–733

Pugh PR (1975) The distribution of siphonophores in a transect across the North Atlantic Ocean at 32°N. J Exp Mar Biol Ecol 20:77–97

Pugh PR (1984) The diel migrations and distributions within a mesopelagic community in the North East Atlantic. 7. Siphonophores. Prog Oceanogr 13:461–489

R Core Team (2019) R: a language and environment for statistical computing. R Foundation for statistical computing, Vienna

Richards WJ (2005) Early stages of Atlantic fishes: an identification guide for the western central north Atlantic, Two Volume Set, CRC Press.

Roe H, Badcock J (1984) The diel migrations and distributions within a mesopelagic community in the North East Atlantic. 5. Vertical migrations and feeding of fish. Prog Oceanogr 13: 389–424

Romero-Romero S, Choy CA, Hannides CCS, Popp BN, Drazen JC (2019) Differences in the trophic ecology of micronekton driven by diel vertical migration. Limnol Oceanogr 64:1473–1483

Ross SW, Quattrini AM, Roa-Varón AY, McClain JP (2010) Species composition and distributions of mesopelagic fishes over the slope of the north-central Gulf of Mexico. Deep-Sea Res II 57:1926–1956

Ryan TE, Downie RA, Kloser RJ, Keith G (2015) Reducing bias due to noise and attenuation in open-ocean echo integration data. ICES J Mar Sci 72:2482–2493

Saba GK, Burd AB, Dunne JP, Hernández-León S, Martin AH, Rose KA, Salisbury J, Steinberg DK, Trueman CN, Wilson RW, Wilson SE (2021) Toward a better understanding of fish-based contribution to ocean carbon flux. Limnol Oceanogr 66:1639–1664

Saenger RA (1989) Bivariate normal swimbladder size allometry models and allometric exponents for 38 mesopelagic swimbladdered fish species commonly found in the North Sargasso Sea. Can J Fish Aquat Sci 46:1986–2002

Sevilla RG, Diez A, Norén M, Mouchel O, Jérôme M, Verrez-Bagnis V, Van Pelt H et al (2007) Primers and polymerase chain reaction conditions for DNA barcoding teleost fish based on the mitochondrial cytochrome b and nuclear rhodopsin genes. Mol Ecol Notes 7: 730–734

Simmonds J, MacLennan DN (2006) Fisheries acoustics: theory and practice, Wiley.

St. John MA, Borja A, Chust G, Heath M, Grigorov I, Mariani P, Martin AP et al (2016) A dark hole in our understanding of marine ecosystems and their services: perspectives from the mesopelagic community. Front Mar Sci 3:31

Stanton TK, Chu D, Wiebe PH, Martin LV, Eastwood RL (1998) Sound scattering by several zooplankton groups. I. Experimental determination of dominant scattering mechanisms. J Acoust Soc Am 103: 225–235

Steinberg DK, Carlson CA, Bates NR, Johnson RJ, Michaels AF, Knap AH (2001) Overview of the US JGOFS Bermuda Atlantic Time-series Study (BATS): a decade-scale look at ocean biology and biogeochemistry. Deep-Sea Res II 48: 1405–1447

Sutton TT (2013) Vertical ecology of the pelagic ocean: classical patterns and new perspectives. J Fish Biol 83:1508–1527

Sutton TT, Porteiro FM, Heino M, Byrkjedal I, Langhelle G, Anderson CIH, Horne J et al (2008) Vertical structure, biomass and topographic association of deep-pelagic fishes in relation to a mid-ocean ridge system. Deep-Sea Res II 55:161–184

Sutton TT, Wiebe PH, Madin L, Bucklin A (2010) Diversity and community structure of pelagic fishes to 5000m depth in the Sargasso Sea. Deep-Sea Res II 57:2220–2233

Sutton TT, Clark MR, Dunn DC, Halpin PN, Rogers AD, Guinotte J, Bograd SJ et al (2017) A global biogeographic classification of the mesopelagic zone. Deep Sea Res I 126:85–102

Walsh PS, Metzger DA, Higuchi R (1991) Chelex 100 as a medium for simple extraction of DNA for PCR-based typing from forensic material. Biotechniques 10:506–513

Whitehead PJP, Bauchot ML, Hureau JC, Nielsen J, Tortonese E (1986) Fishes of the North-Eastern Atlantic and the Mediterranean. Three Volume Set. UNESCO publication, Paris.

Wienerroither R, Uiblein F, Bordes F, Moreno T (2009) Composition, distribution, and diversity of pelagic fishes around the Canary Islands, Eastern Central Atlantic. Mar Biol Res 5:328–344